Enhancing Mechanical Properties of Sustainable Thermoplastic Elastomers through Incorporating Ionic Interactions

Wenyue Ding,[a 1] *Josiah Hanson,*[a 1], *Yi Shi,*[b 2] *Yan Yao,*[b] *and Megan L. Robertson*[ac]*

[a] William A. Brookshire Department of Chemical & Biomolecular Engineering, University of Houston, Houston, TX, 77204
[b] Department of Electrical and Computer Engineering, University of Houston, Houston, Texas 77204
[c] Department of Chemistry, University of Houston, Houston, TX, 77204

[1] These authors contributed equally to this work
[2] Current address: School of Materials Science and Engineering, Sun Yat-Sen University, Guangzhou 510275, China.

*Corresponding author
Megan Robertson
4226 Martin Luther King Blvd.
S222 Engineering Building 1
University of Houston
Houston, TX 77204-4004
mlrobertson@uh.edu
713-743-2748

TOC Graphic:

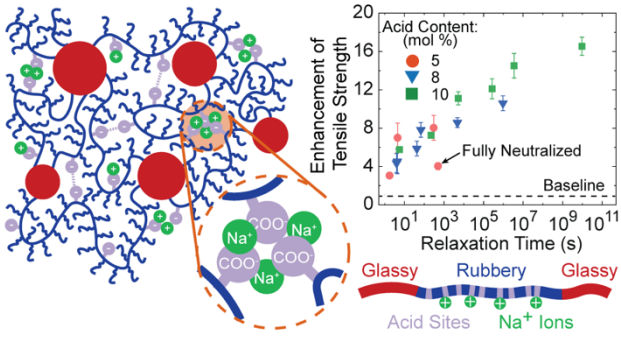

Keywords: Ionomer Midblock, Fatty Acid, Vegetable Oil, Transient Interactions, Supramolecular Interactions, Supramolecular Network, Dynamic Crosslinks, Long-Chain Polyacrylates, Hydrogen Bonding

Abstract

The physical properties of an ABA triblock copolymer-based thermoplastic elastomer, containing a poly(lauryl methacrylate-*co*-methacrylic acid) midblock and poly(methyl methacrylate) endblocks, were enhanced through neutralization of the methacrylic acid (MAA) repeat units with NaOH to form ionic interactions in the midblock. Rheological properties of the midblock and mechanical properties of the triblock copolymer were investigated as functions of acid (MAA) and ion content. Midblock relaxation times (τ) increased with increasing acid and ion content, however the activation energy extracted from an Arrhenius analysis appeared constant for all acid and ion contents. Meanwhile, the factors of enhancement of the strain at break and tensile strength (as compared to the baseline polymer without ionic interactions or hydrogen bonding) collapsed onto master curves when plotted as functions of $\log \tau$, indicating the mechanical behavior of the triblock copolymer could be tuned through varying the relaxation time of the midblock. The tensile strength increased by as much as a factor of 17 times greater than that of the baseline polymer. More moderate enhancements were observed in the strain at break, with the maximum strain at break occurring at intermediate relaxation times. This suggests that midblock chain dynamics are a governing factor for the mechanical property enhancements, due to the effects of the ionic aggregates and chain mobility on stress dissipation under tensile deformation.

Introduction

Thermoplastic elastomers (TPEs) are a class of polymer characterized by a rubbery matrix that contains physical crosslinks due to the presence of hard, dispersed domains bridged by the softer rubbery material.[1] TPEs can have the advantages of both conventional crosslinked elastomers (e.g., extensibility, flexibility and resilience) and thermoplastics (e.g., processability and recyclability) and have been widely used in a variety of applications such as automotive components, footwear, medical devices and sporting goods due to their unique properties.[1-4] The vast majority of TPEs are produced from petroleum-based feedstocks, which is of growing concern due to the finite nature of the resource as well as the significant negative environmental and health related challenges associated with petroleum products.[5-7] As such, there has been enormous efforts made towards the development of more sustainable and renewable TPEs. There has been notable success in producing a wide variety of building blocks that can be derived from various sustainable and renewable feedstocks such as: vegetable oils and their fatty acids,[8-10] sugars,[11-14] rosin,[15, 16] lignin,[17, 18] terpenes,[19-21] and more. However, the creation of such a library of sustainable building blocks is only the first step towards development of sustainable TPEs. The widespread adoption of sustainable TPEs requires competitive, if not superior, material performance compared to petroleum-based products.

The most common TPEs are those that utilize an ABA triblock copolymer structure with hard and glassy A endblocks (typically polystryrene) and a soft rubbery B midblock (polyisoprene, butadiene, ethylene-*co*-butylene, etc.) which make up 45-50% of the TPE market.[22, 23] One important factor that impacts the mechanical properties of triblock copolymer TPEs is the polymer chemical structure and its ability to form entanglements.[24, 25] Entanglements play a crucial role in the failure mechanism of triblock copolymer TPEs as they allow for better stress dissipation

throughout the material.[24, 26] Without entanglements, stress is more greatly concentrated on a smaller number of physical crosslinks, leading to chain pull-out and break down of the physical crosslinks, ultimately leading to material failure.[24, 26] Unfortunately, many alternative bio-based polymers that are suitable for use as the soft midblock of ABA triblock copolymer TPEs contain bulky moieties, preventing entanglements and severely hindering their mechanical performance.[10, 24, 27-29] There has been some success with developing linear midblock structures using terpenes derived from mint plants as well as a ring opening polymerization of renewable lactones to produce higher performing TPEs.[30, 31] However, due to the wide array of TPE applications, it is desirable to produce sustainable TPEs from a variety of different sources, producing a library of polymers and increasing the range of achievable material properties. Thus, developing methods that enable the use of a diverse array of biobased TPEs without hampering performance is imperative.

One attractive approach that has been of increasing interest for achieving enhanced mechanical performance in ABA triblock copolymer TPEs (among other architectures)[32-40] has been the incorporation of a variety of dynamic and transient interactions such as hydrogen bonding, metal-ligand coordination, π-π stacking and ionic interactions.[14, 41-63] These types of transient interactions can act as dynamic crosslinks, enhancing the mechanical properties of the TPE, or can even add new dynamic properties to the TPE that were not already present. Hydrogen bonding groups have been incorporated in both mid- and endblocks using a wide variety of chemical groups, such as amide groups, hydroxyl groups, complementary adenine and thymine nucleobases, quadruple hydrogen bonding 2-ureido-4-pyrimidinone groups, which have resulted in significant improvements in tensile strength and modulus and self-healing properties.[14, 42, 47-49, 51-56, 64] Metal-ligand interactions have similarly been introduced in various TPE systems to enhance mechanical behavior, as well as impart shape memory, self-healing, or luminescence to the material.[38, 43, 46, 57,

[65] Metal-ligand interactions also offer additional dimensions of property tuning due to the large number of metal-ligand complexes that could be utilized. However, the use of environmentally hazardous transition metals is required. Additionally, π- π stacking has largely been incorporated as a secondary interaction between groups undergoing other dynamic interactions like hydrogen bonding or metal-ligand coordination that also involves aromatic rings.[55, 58, 59]

Ionic interactions also offer significant opportunities in tuning material properties due to numerous choices of ion pairs. Ionic interactions have been less explored in TPEs as compared to hydrogen bonding or metal-ligand complexes, despite showing similar performance enhancements.[41, 44, 45, 60-63] For example, a triblock copolymer containing poly(*n*-butyl acrylate)-*co*-poly(1-vinylimidazole) was produced, where the imidazole groups were further ionically crosslinked by 1,6-dibromohexane, which showed improvements in ultimate tensile strength and elastic recovery due to the presence of ionic crosslinker.[45] Triblock copolymers with poly(4-vinyl pyridine) (P4VP) as the hard segment exhibited great improvements in Young's modulus, tensile strength, and toughness as a result of zinc-pyridine interactions.[63] Additionally, a recent study demonstrated a high-performance, recyclable TPE utilizing Zn-neutralized carboxylates and poly(carbonate-esters), achieving tensile strength of 60 MPa and strain at break of 800%.[41, 44] As such, there lies great opportunity in utilizing ionic interactions in the development of sustainable triblock copolymer TPEs who otherwise suffer from poor mechanical performance. Currently, there have been only a few reports on biobased triblock copolymer TPEs with transient interactions, with most utilizing hydrogen bonding[14, 42, 48, 49, 52] and very few using metal-ligand interactions[43, 46] or ionic interactions.[41, 44, 45]

Our group has been investigating the use of poly(meth)acrylates derived from fatty acids as biobased midblocks in triblock copolymer TPEs.[10, 16, 27, 48, 66, 67] Fatty acids contain anywhere

from 12-20 carbon atoms, and poly(meth)acrylates derived from fatty acids have long alkyl side chains (carbon length n = 12-20) which lead to exceedingly high entanglement molecular weights.[68, 69] This class of polymers is typically unentangled at accessible molecular weights. This limits the mechanical performance of triblock copolymers that contain fatty acid-based poly(meth)acrylate midblocks.[10, 27-29] We have previously demonstrated the incorporation of hydrogen bonding groups into the midblock, which significantly improved the tensile strength and strain at break of the triblock copolymers.[48] Here, we extend this approach to the incorporation of ionic interactions, due to the versatility and tunability of the ionic groups. To our knowledge, the application of ionic interactions as a transient network in the midblock of a biobased ABA triblock copolymer TPE has not been previously examined. In our study, triblock copolymers were synthesized with lauric acid-based poly(lauryl methacrylate) midblocks and poly(methyl methacrylate) endblocks. Ionic interactions were incorporated into the midblock through use of a (*tert*-butyl methacrylate) comonomer in the midblock (in the range of 5-10 mol%), which was hydrolyzed to methacrylic acid (capable of forming hydrogen bonds) and subsequently neutralized with sodium hydroxide to introduce ionic crosslinks into the system. Na^+ was chosen as the neutralizing cation for this study due to its high mobility compared to other ions and simple electronic structure which reduces the occurrence of more complex ionic coordination states,[70-74] which may lead to a clearer view of how the presence of the ions impacts chain relaxation behavior. Enhancements in tensile strength and strain at break of the triblock copolymer were examined as functions of acid and ion content of the midblock. The role of chain dynamics in the midblock, as characterized by the relaxation time through rheology, was probed. This work provides valuable insight into the fundamental relationships among mechanical property enhancements, chain

dynamics, and transient network formation (via ionic interactions and hydrogen bonding in the midblock) in these materials.

Experimental Methods

Materials

All chemicals were purchased from Sigma Aldrich unless otherwise noted.

Synthesis of Bifunctional RAFT Agent

The RAFT agent ethane-1,2-diyl bis(4-cyano-4-(((dodecylthio)carbonothioyl)thio)pentanoate) was produced using the following procedure. First, ethylene glycol (0.22 g, 3.6 mmol), 4-cyano-4-[(dodecylsulfanylthiocarbonyl)sulfanyl]pentanoic acid (3.2 g, 7.9 mmol), and DMAP (0.22 g, 1.8 mmol) were dissolved in 15 mL of dried dichloromethane (DCM). Then, N-(3-Dimethylaminopropyl)-N′-ethylcarbodiimide hydrochloride (EDC•HCl) (2.81 g, 14.4 mmol) was added while stirring. After 24 hours, 50 mL of DCM was added into the solution, which was washed with NaCl solution three times. The DCM phase was dried over MgSO4 and, after filtration, the crude product was purified by flash chromatography (silica gel, petroleum ether/chloroform = 1:3). The product was dried at room temperature in a vacuum to give 2.4 g of product (yield 70%).

Synthesis of Poly(lauryl methacrylate-*co*-methacrylic acid) [P(LMA-*co*-MAA)] Copolymers

Poly(lauryl methacrylate-*co*-methacrylic acid) [P(LMA-*co*-MAA)] copolymers were prepared by first synthesizing poly(lauryl methacrylate-*co*-*tert* butyl methacrylate) (P(LMA-*co*-*t*BMA)) copolymers and subsequently hydrolyzing to P(LMA-*co*-MAA) (**Scheme 1**). P(LMA-*co*-*t*BMA) copolymers were synthesized by reversible addition-fragmentation chain-transfer (RAFT) polymerization using the chain transfer agent 4-cyano-4-[(dodecylsulfanylthiocarbonyl)sulfanyl]pentanoic acid. LMA and *t*BMA monomers were passed

through a basic aluminum oxide column to remove monomethyl ether hydroquinone inhibitor. As an example, the copolymer containing 10 mol% P*t*BMA was prepared as follows. LMA (40 g, 0.16 mol), *t*BMA (2.4 g, 0.017 mol), 4-cyano-4-[(dodecylsulfanylthiocarbonyl)sulfanyl]pentanoic acid (126 mg, 0.31 mmol), azobisisobutyronitrile (AIBN) (10.4 mg, 0.06 mmol) and 1,4-dioxane (26 mL) were added to a round bottom flask. The flask was sealed with a rubber septum, purged with argon for 30 min, and immersed into an oil bath at 70°C and left stirring for 16 hours. The reaction was then quenched by cooling with cold water and the P(LMA-*co*-*t*BMA) copolymers were precipitated into methanol three times, followed by drying in a vacuum oven at 40 °C overnight. P(LMA-*co*-*t*BMA) copolymers with different *t*BMA content were synthesized by changing the feed ratio of LMA to *t*BMA. P(LMA-*co*-*t*BMA) copolymers are referred to as $P(LMA_{100-x}\text{-}co\text{-}tBMA_x)$, where x is the mol% of *t*BMA in the copolymer.

P(LMA-*co*-*t*BMA) was then hydrolyzed with trifluoracetic acid to form P(LMA-*co*-MAA) copolymers. In a round bottom flask, P(LMA-*co*-*t*BMA) (36g) was dissolved in 280 mL dichloromethane. Under vigorous stirring, 20 mL trifluoracetic acid (98%) was added dropwise into the solution and the reaction was carried out at room temperature for 36 hours. The solution was then concentrated and precipitated into methanol, followed by drying in a vacuum oven at 40°C overnight. P(LMA-*co*-MAA) copolymers are referred to as $P(LMA_{100-y}\text{-}co\text{-}MAA_y)$, where y is the mol% of MAA in the copolymer.

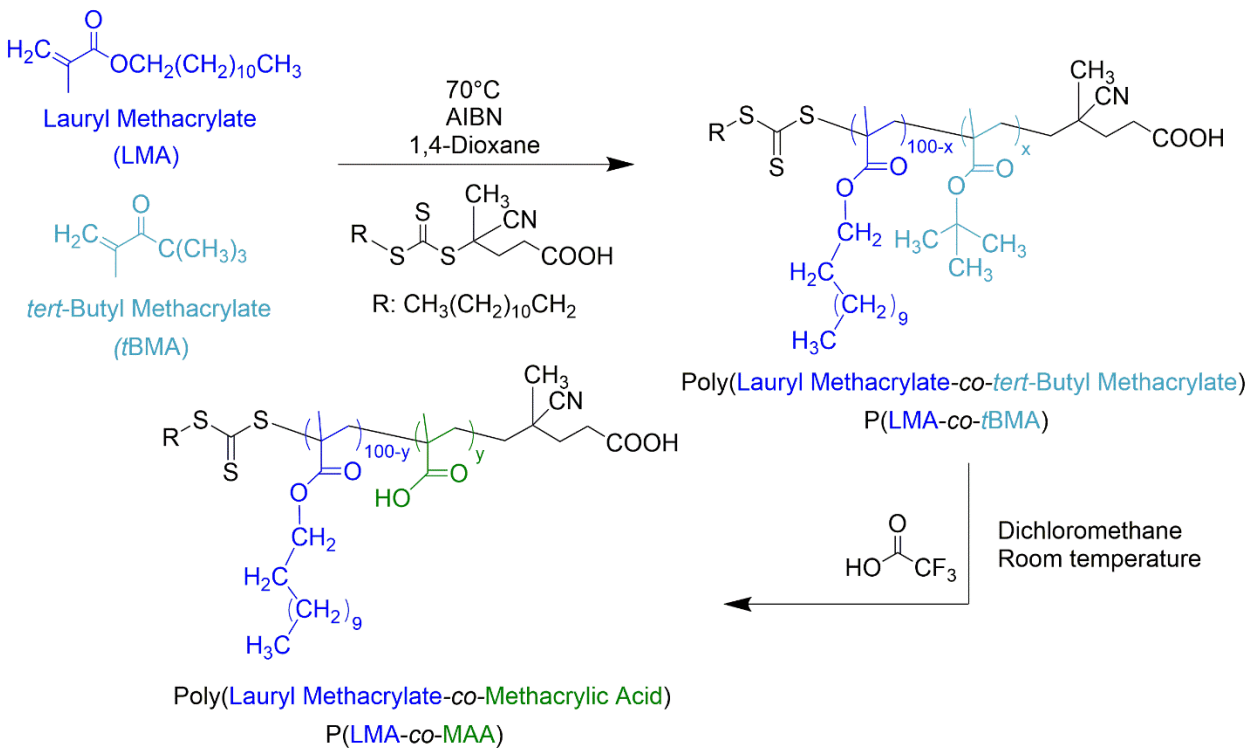

Scheme 1. Synthesis of P(LMA-*co*-MAA) copolymers through RAFT polymerization. x is the mol% of *t*BMA in the P(LMA-*co*-*t*BMA) copolymer and y is the mol% of MAA in the P(LMA-*co*-MAA) copolymer.

Synthesis of Poly(methyl methacrylate-*b*-(lauryl methacrylate-*co*-methacrylic acid)-*b*-methyl methacrylate (PMMA-*b*-P(LMA-*co*-MAA)-*b*-PMMA) Triblock Copolymers

Poly(methyl methacrylate-*b*-(lauryl methacrylate-*co*-methacrylic acid)-*b*-methyl methacrylate (PMMA-*b*-P(LMA-*co*-MAA)-*b*-PMMA) triblock copolymers were prepared by first synthesizing poly(methyl methacrylate-*b*-(lauryl methacrylate-*co*-*tert*-butyl methacrylate)-*b*-methyl methacrylate (PMMA-*b*-P(LMA-*co*-*t*BMA)-*b*-PMMA) triblock copolymers and subsequently hydrolyzing to PMMA-*b*-P(LMA-*co*-MAA)-*b*-PMMA (**Scheme 2**). PMMA-*b*-P(LMA-*co*-*t*BMA)-*b*-PMMA was synthesized through a two-step RAFT polymerization. P(LMA-*co*-*t*BMA) was synthesized using bifunctional RAFT agent ethane-1,2-diyl bis(4-cyano-4-(((dodecylthio)carbonothioyl)thio)pentanoate). As one example, the copolymer containing 10 mol% P*t*BMA was prepared as follows: LMA (40 g, 0.16 mol), *t*BMA (2.4 g, 0.017 mol),

bifunctional RAFT agent (264 mg, 0.31 mmol), AIBN (10.4 mg, 0.06 mmol) and 1,4-dioxane (26 mL) were added to a round bottom flask. The flask was then sealed with a rubber septum, purged with argon for 30 min and immersed into an oil bath at 70°C and left stirring for 16 hours. The reaction was then quenched by cooling with cold water and the bifunctional P(LMA-*co*-*t*BMA) copolymers were precipitated into methanol three times followed by drying in a vacuum oven at 40 °C overnight. Then, PMMA-*b*-P(LMA-*co*-*t*BMA)-*b*-PMMA triblock copolymers were synthesized by chain extension of bifunctional P(LMA-*co*-*t*BMA) midblock with MMA monomer. MMA monomer was passed through a basic alumina oxide column to remove monomethyl ether hydroquinone inhibitor. A typical procedure is as follows: MMA (16 g, 0.159 mol), bifunctional P(LMA-*co*-*t*BMA) copolymer (38 g, 0.37 mmol), AIBN (12 mg, 0.07 mmol) and 1,4-dioxane (120 mL) were added to a round bottom flask. The flask was then sealed with a rubber septum, purged with argon for 30 min and immersed into an oil bath at 70°C and left stirring for 20 hours. The reaction was quenched by cooling with cold water and the copolymers were precipitated into methanol three times followed by drying in a vacuum oven at 100 °C overnight. PMMA-*b*-P(LMA-*co*-*t*BMA)-*b*-PMMA triblock copolymers are referred to as PMMA-*b*-P(LMA_{100-x}-*co*-$tBMA_x$)-*b*-PMMA triblock copolymers, where x is the mol% of *t*BMA in the midblock.

PMMA-*b*-P(LMA-*co*-*t*BMA)-*b*-PMMA triblock copolymers were hydrolyzed with trifluoracetic acid to form PMMA-*b*-P(LMA-*co*-MAA)-*b*-PMMA triblock copolymers. In a round bottom flask, PMMA-*b*-P(LMA-*co*-*t*BMA)-*b*-PMMA (42 g) was dissolved in 280 mL dichloromethane (BDH, ACS grade). Under vigorous stirring, 20 mL trifluoracetic acid (98%) was added dropwise into the solution and the reaction was carried out at room temperature for 36 hours. The solution was then concentrated and precipitated into methanol followed by drying in a vacuum

oven at 100 °C overnight. PMMA-*b*-P(LMA-*co*-MAA)-*b*-PMMA triblock copolymers are referred to as PMMA-*b*-P(LMA$_{100-y}$-*co*-MAA$_y$)-*b*-PMMA, where y is the mol% of MAA in the midblock.

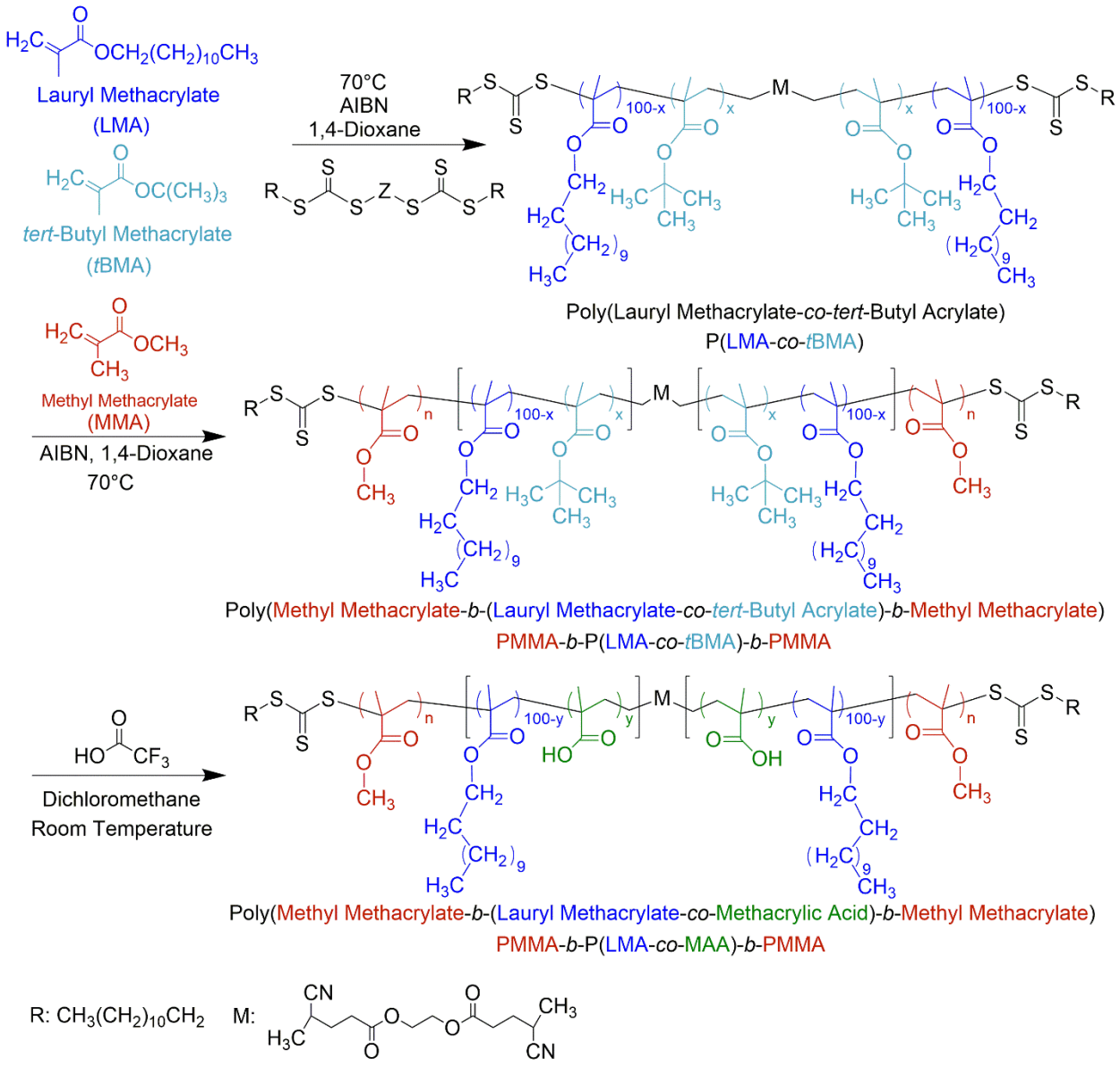

Scheme 2. Synthesis of PMMA-*b*-P(LMA-*co*-MAA)-*b*-PMMA triblock copolymers through RAFT polymerization.

Neutralization of Acid Groups to Form Ionic Groups

The P(LMA-*co*-MAA) copolymers and PMMA-*b*-P(LMA-*co*-MAA)-*b*-PMMA triblock copolymers were neutralized with NaOH to varying degrees. For example, the P(LMA_{90}-*co*-MAA_{10}) copolymer with 5 mol% ion content was prepared as follows: P(LMA_{90}-*co*-MAA_{10}) (6 g) was dissolved in 20 ml THF in a round bottom flask. 1.3 mL of NaOH/methanol solution (39 mg/mL) was added to the flask under vigorous stirring. The neutralization was then carried out at room temperature for 24h. After that, the mixture was poured into a Teflon mold, left in fume hood for 24h, and then dried in vacuum oven at 40 °C overnight. Following partial or full neutralization of MAA repeat units, P(LMA-*co*-MAA) is referred to as P($LMA_{100-y-z}$-*co*-MAA_y-*co*-MAA_z^{Na}) where y is the mol% of un-neutralized MAA in the copolymer and z is the ion content (mol% of Na-neutralized MAA repeat units in the copolymer). Following partial or full neutralization of MAA repeat units, PMMA-*b*-P(LMA-*co*-MAA)-*b*-PMMA is referred to as PMMA-*b*-P($LMA_{100-y-z}$-*co*-MAA_y-*co*-MAA_z^{Na})-*b*-PMMA where y is the mol% of un-neutralized MAA in the midblock and z is the ion content (mol% of Na-neutralized MAA repeat units in the midblock).

Nuclear Magnetic Resonance (NMR)

^{1}H NMR experiments were performed with a JEOL ECA-400 instrument using deuterated chloroform (99.96 atom % D) as the solvent. Chemical shifts were referenced to the residual protonated solvent resonance (7.24 ppm). ^{13}C NMR experiments were performed with a JEOL ECA-600 II instrument using deuterated chloroform (99.96 atom % D) as the solvent. The relaxation delay was set to 10 s and nuclear Overhauser effect (NOE) was turned off. Chemical shifts were referenced to the residual protonated solvent resonance (77.1 ppm)

Gel Permeation Chromatography (GPC)

Number-average molecular weight (M_n) and dispersity ($Đ$) were measured using a Viscotek gel permeation chromatography (GPC) instrument, with two Agilent ResiPore columns using THF (OmniSolv, HPLC grade) as the mobile phase at 30 °C. The flow rate was 1 mL/min with an injection volume of 100 μL. A triple detection system, consisting of a light scattering detector, a viscometer, and refractometer, was employed to characterize the absolute molecular weight.

Fourier-Transform Infrared Spectroscopy (FTIR)

FTIR spectra were obtained using a Thermo Scientific Nicolet 4700 spectrometer. Thin films of polymers were prepared by solvent casting from 1% (w/v) solution in dichloromethane (J.T. Baker, OmniSolv, HPLC grade) onto potassium bromide (KBr) windows (32 mm diameter, 3 mm thickness). The sample was air-dried for an hour and then transferred to a vacuum oven to remove residual solvent by drying *in vacuo* for 24 hours. After drying, the sample was mounted to a sample holder and the spectra was recorded using 64 scans at a resolution of 4 cm^{-1} in transmission mode.

Rheology

The viscoelastic behavior of P(LMA-*co*-*t*BMA) and P(LMA-*co*-MAA) copolymers was evaluated using a TA instruments DHR-2 rheometer with 25 mm diameter parallel plates, and a sample thickness of 1 mm. The linear viscoelastic region was first determined through measurement of the storage (G') and loss (G'') moduli using a strain sweep from 1 – 10% strain at a frequency (ω) of 10 rad/s. The moduli were then measured at a strain within the linear region, over a range of frequencies (ω = 0.1 – 100 rad/s), measured every 10 °C. Time-temperature superposition at a reference temperature of 30 °C was performed using TA Instruments TRIOS software to generate master curves.

Mechanical Properties

Tensile testing was conducted using an Instron 5966 universal testing system with a 100 N load cell at a grip speed of 10 mm/min. Dog bone-shaped testing bars (following ASTM D638, bar type 5, thickness 1.5 mm) were prepared by compression molding on a Carver Hotpress at an applied load of 4200 lbs at 180 °C. Pneumatic grips (maximum 2 kN) were used to affix the sample in the testing frame, at a compressed air pressure of 35 psi. The measurements were repeated with 5 test specimens.

Results and Discussion

Triblock copolymers were synthesized with a lauric acid-based poly(lauryl methacrylate) (PLMA) midblock and poly(methyl methacrylate) (PMMA) endblocks. Ionic interactions were incorporated into the midblock through use of a *tert*-butyl methacrylate (*t*BMA) comonomer in the midblock (in the range of 5-10 mol%), which was hydrolyzed to methacrylic acid (MAA, capable of forming hydrogen bonds) and subsequently neutralized with sodium hydroxide to introduce ionic crosslinks into the system. Na^+ was chosen as the neutralizing cation for this study due to its high mobility compared to other ions and simple electronic structure which reduces the occurrence of more complex ionic coordination states,[70-74] which may lead to a clearer view of how the presence of the ions impacts chain relaxation behavior.

Synthesis and Neutralization of P(LMA-*co*-MAA) Copolymers

P(LMA-*co*-*t*BMA) copolymers were synthesized through RAFT polymerization and then hydrolyzed to form P(LMA-*co*-MAA) copolymers (**Scheme 1**). To create ionically crosslinked copolymers, P(LMA-*co*-MAA) copolymers were neutralized with NaOH. Three series of P(LMA-*co*-MAA) copolymers were synthesized, each containing different acid (MAA) content (5, 8 and 10 mol%). Within each series of differing acid (MAA) content, the ion content (z, mol% of Na-neutralized MAA repeat units in the midblock) was varied between 0 and 5 mol%. All the P(LMA-*co*-MAA) copolymers had similar molecular weight (106 – 110 kg/mol) and dispersity (Đ: 1.3-1.4). Polymer characteristics are summarized in **Table S1**.

The composition of P(LMA-*co*-*t*BMA) copolymers was confirmed using NMR (**Figure 1**). Characteristic peaks associated with the methylene groups on the carbon side-chain of the LMA repeat units are observed at 1.3 ppm (labeled g, h, i), 1.6 ppm (labeled f) and 3.9 ppm (labeled e) in **Figure 1a**. Peaks associated with the methyl groups of the *t*BMA repeat units are observed at

1.4 ppm (labeled k). Due to peak overlap, we turned to ^{13}C NMR to quantify the mol% of *t*BMA in P(LMA-*co*-*t*BMA) copolymers (**Figure 1b**). The areas of peaks associated with methyl groups on *t*BMA (peak k at 27.8 ppm) and of LMA (peak j at 14.2 ppm) were used to calculate the mol% of *t*BMA:

$$\text{mol\% } t\text{BMA} = \frac{A_k/3}{A_j + A_k/3} * 100 \qquad \text{(eq. 1)}$$

where A_k and A_j are peak areas for carbons k and j respectively. M_n and Đ were characterized with GPC (**Table S1**); the polymers exhibited monomodal distributions (**Figure S1)** with relatively low dispersity (Đ: 1.2-1.3), indicating the RAFT polymerization of P(LMA-*co*-*t*BMA) copolymers was well controlled.

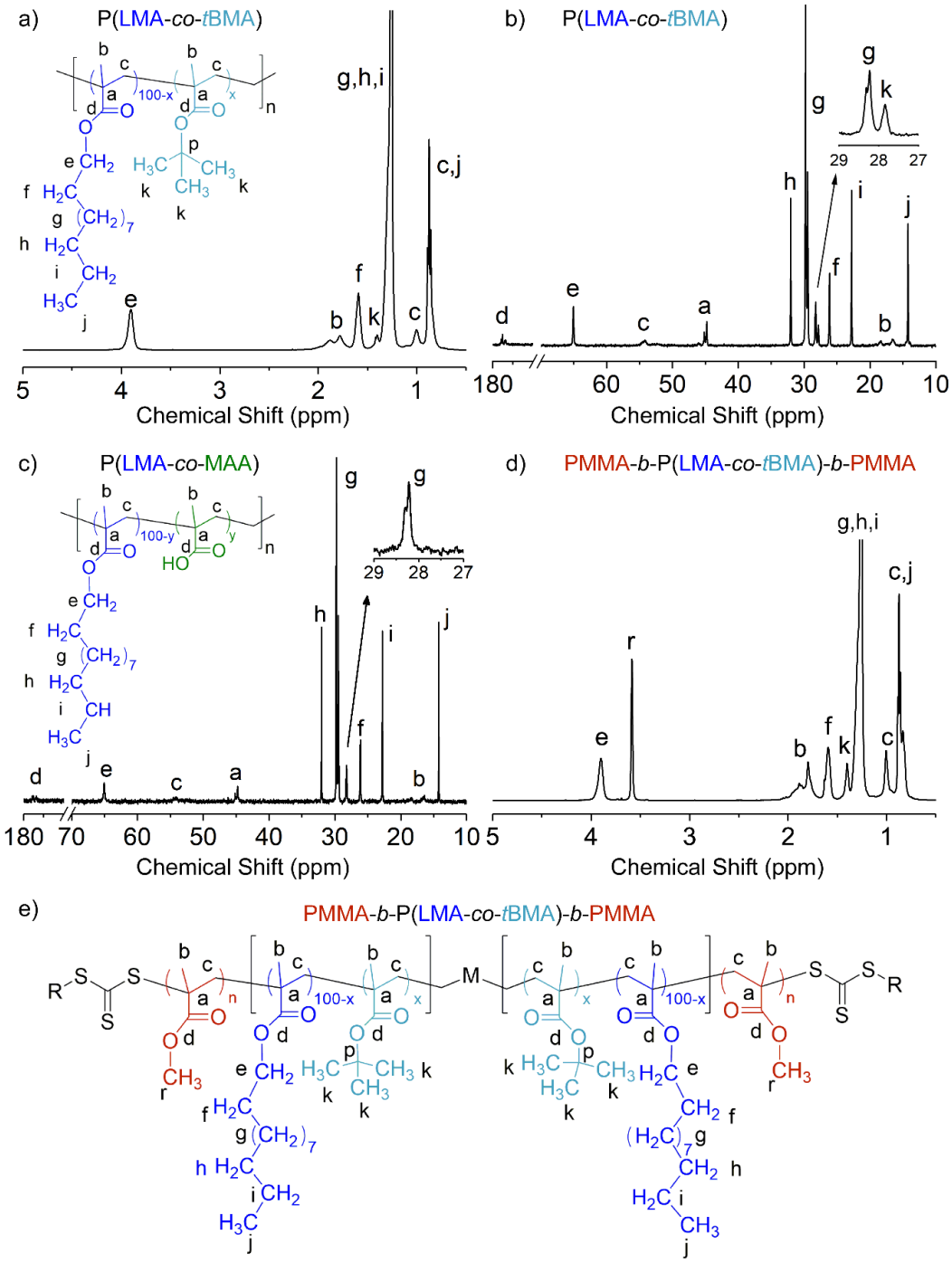

Figure 1. (a) ^{1}H and (b) ^{13}C NMR data obtained from P(LMA$_{90}$-*co*-*t*BMA$_{10}$) (the same peak labels are used in both figures). (c) ^{13}C NMR data obtained from P(LMA$_{90}$-*co*-MAA$_{10}$). (d) ^{1}H NMR data obtained from PMMA-*b*-P(LMA$_{90}$-*co*-*t*BMA$_{10}$)-*b*-PMMA, with peak labels shown in (e).

The P(LMA-*co*-*t*BMA) copolymers were hydrolyzed with trifluoroacetic acid to form P(LMA-*co*-MAA) copolymers. *t*BMA repeat units were fully hydrolyzed to MAA as confirmed by ^{13}C NMR (**Figure 1c**), where the characteristic peak at 27.8 ppm corresponding to methyl groups on the tBMA side-chain disappeared completely. Thus, the mol% MAA in P(LMA-*co*-MAA) was the same as the mol% *t*BMA in the parent P(LMA-*co*-*t*BMA) copolymer.

P(LMA-*co*-MAA) copolymers were then neutralized with NaOH to form ionically crosslinked copolymers, P($LMA_{100-y-z}$-*co*-MAA_y-*co*-MAA_z^{Na}) where y is the mol% of un-neutralized MAA and z is the ion content (mol% of Na-neutralized MAA) in the copolymer. The ion content was varied by modifying the amount of NaOH used, and quantified through FTIR. FTIR spectra obtained from P(LMA_{92}-*co*-MAA_{8-z}-*co*-MAA_z^{Na}) are shown in **Figure 2**. Peaks corresponding to C=O stretching of LMA and MAA are observed at 1732 and 1700 cm^{-1}, respectively, for all samples. Upon neutralization, the intensity of the peak corresponding to the C=O bond of MAA at 1700 cm^{-1} decreased and a new peak corresponding to the neutralized acid group COO^- at 1575 cm^{-1} was identified, indicating a portion of the acid groups in MAA were successfully neutralized. The mol% of Na-neutralized MAA in the copolymer (z) was calculated from reduction of peak intensity at 1700 cm^{-1} using:

$$z = \frac{I_{\text{pre-neutralized}} - I_{\text{neutralized}}}{I_{\text{pre-neutralized}}} * \text{mol\% MAA} \qquad \text{(eq. 2)}$$

where $I_{\text{pre-neutralized}}$ is that of the P(LMA-*co*-MAA) copolymer prior to neutralization, $I_{\text{neutralized}}$ is that of P($LMA_{100-y-z}$-*co*-MAA_y-*co*-MAA_z^{Na}) following neutralization to ion content z, and mol% MAA is the mol% of MAA repeat units in the P(LMA-*co*-MAA) copolymer prior to neutralization. The results are tabulated in **Table S1**.

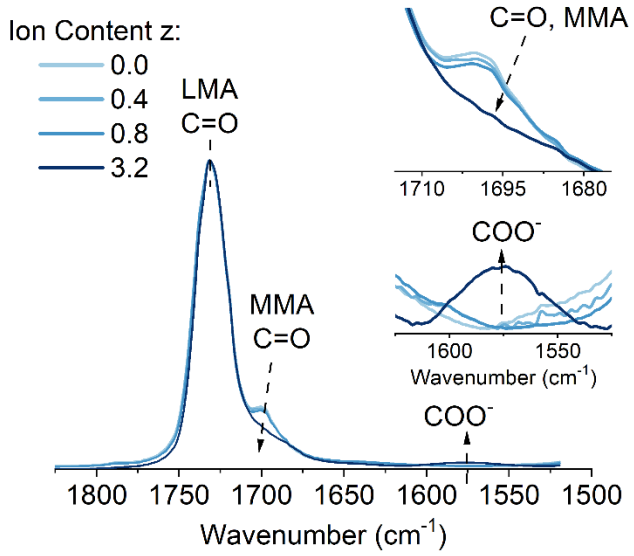

Figure 2. FTIR spectra obtained from P(LMA$_{92}$-*co*-MAA$_{8-z}$-*co*-MAA$_z^{Na}$) where z is the ion content (mol% of Na-neutralized MAA) in the copolymer. Peaks were normalized to the C=O stretching band of LMA. Insets highlight decreasing shoulder peak intensity at approximately 1700 cm^{-1} (top) and peak formation at approximately 1575 cm^{-1} (bottom) with increasing ion content.

Synthesis and Neutralization of PMMA-*b*-P(LMA-*co*-MAA)-*b*-PMMA Triblock Copolymers

Ionic PMMA-*b*-P(LMA-*co*-MAA)-*b*-PMMA triblock copolymers were synthesized using a two-step RAFT polymerization followed by hydrolysis and neutralization (**Scheme 2**). The midblock P(LMA-*co*-*t*BMA) was synthesized using a bifunctional chain transfer agent and then chain extended with MMA to form PMMA-*b*-P(LMA-*co*-*t*BMA)-*b*-PMMA triblock copolymers. Then, PMMA-*b*-P(LMA-*co*-*t*BMA)-*b*-PMMA triblock copolymers were hydrolyzed to form PMMA-*b*-P(LMA-*co*-MAA)-*b*-PMMA, followed by neutralization with NaOH to generate ionically crosslinked triblock copolymers. Three series of PMMA-*b*-P(LMA-*co*-MAA)-*b*-PMMA triblock copolymers were synthesized, each containing different acid (MAA) content in the midblock (5, 8 and 10 mol%). Within each series, ion content (z) was varied in a corresponding manner to that of the P(LMA-*co*-MAA) samples (**Table S2**). All the triblock copolymers had similar overall molecular weight (125 – 136 kg/mol), wt% of PMMA endblocks (18-22 wt%) and dispersity Đ (1.4) (shown in **Table S2**).

The composition and M_n of the bifunctional P(LMA-*co*-*t*BMA) midblock was characterized using the same methods as discussed previously. Following chain extension of the P(LMA-*co*-*t*BMA) midblock with MMA to form PMMA-*b*-P(LMA-*co*-*t*BMA)-*b*-PMMA triblock copolymers, ^{1}H NMR confirmed incorporation of PMMA endblocks, with peaks observed at 3.6 ppm corresponding to –OCH_3 on the MMA repeat unit (peak r in **Figure 1d**). Each endblock M_n was determined through knowledge of the midblock M_n and composition (reported in **Table S2**):

$$M_{n,PMMA} = M_{n,\mathrm{P(LMA-}co\mathrm{-}t\mathrm{BMA)}} * \frac{\left(\frac{A_r}{3}\right)*100.12}{\left(\frac{A_e}{2}\right)*254.46+\left(\frac{A_e}{2}\right)\left(\frac{x}{100-x}\right)*142.20} \quad \text{(eq. 3)}$$

in which A_r and A_e are the integration of peaks r and e in **Figure 1d**, x is the mol% of *t*BMA in the midblock characterized through ^{13}C NMR and $M_{n,\mathrm{P(LMA-}co\mathrm{-}t\mathrm{BMA)}}$ is the molecular weight of the P(LMA-*co*-*t*BMA) midblock determined by GPC. All PMMA-*b*-P(LMA-*co*-*t*BMA)-*b*-PMMA triblock copolymers were characterized by GPC, with M_n and $Đ$ summarized in **Table S2**. Upon chain extension, a clear shift of the peak to the left was observed in the GPC refractomer signal (**Figure S1**), further confirming incorporation of PMMA as endblocks. The molecular weight distributions for PMMA-*b*-P(LMA-*co*-*t*BMA)-*b*-PMMA triblock copolymers were bimodal, with a shoulder to the left of the main peak, likely due to bimolecular termination as commonly reported in RAFT polymerization.[75-77] This general phenomenon is typically observed at high monomer conversion or when using a high molecular weight macro-RAFT agent as in our study (the P(LMA-*co*-*t*BMA) macro-RAFT agents had relatively large molecular weight, >100 kg/mol).

Impact of Ionic Interactions on Viscoelastic Properties of P(LMA-*co*-MAA) Copolymers

Dynamics and strength of reversible interactions play key roles in the physical properties of polymers containing dynamic crosslinks (e.g. hydrogen bonds, ionic groups). The dynamic bond lifetime (τ_b), which quantifies the time scale of the bond reversibility, can be probed by quantifying

the relaxation time of the polymer through linear rheology.[78-80] The frequency (ω)-dependent dynamic moduli (G', G'') were characterized at various temperatures for P(LMA-*co*-MAA) copolymers both pre- and post-neutralization with NaOH (as well as for the parent P(LMA-*co*-*t*BMA) copolymers), and time-temperature superposition (TTS) was employed to extend the range of accessible frequencies using a reference temperature of 30 °C (**Figure 3**). TTS was effective for all samples across the accessible temperature range, indicating the presence of a single relaxation mechanism in these materials (shift factors and their fit to the William-Landel-Ferry (WLF) equation (eq. S1) are provided in **Figure S2** and **Tables S3-S7**).

We first discuss the rheological behavior of the P(LMA-*co*-*t*BMA) copolymers, which do not contain dynamic bonds (black data sets in **Figure 3**). All the P(LMA-*co*-*t*BMA) copolymers exhibited Rouse dynamics at high frequency where the slopes of G' and G'' vs ω (on log-log scale) were 1/2, and transitioned to the terminal flow region at low frequencies (with slopes of 1.7-1.9 and 0.9-1.0 for G' and G'', respectively, as tabulated in **Table S8**). Also, the absence of plateau region of G' indicates the P(LMA-*co*-*t*BMA) copolymers remained unentangled, due to the ultra-high entanglement molecular weight M_e of PLMA (M_e = 225 kg/mol[68]). After hydrolysis of *t*BMA to MAA, the *tert*-butyl group was converted to a carboxylic acid group, which can undergo hydrogen bonding. Formation of a dynamic network by hydrogen bonds in P(LMA-*co*-MAA) copolymers increased the moduli as compared to the P(LMA-*co*-*t*BMA) copolymers. Further, as the mol% MAA in the copolymer increased from 5 to 10, the moduli increased due to higher transient crosslink density attributed to the presence of hydrogen bonding (**Figure S3**). Upon neutralization of MAA (quantified by the ion content z, the mol% of Na-neutralized MAA repeat units in the copolymer), the shapes of the master curves generally remained the same with rouse

dynamics observed at high frequencies which then transitioned to the terminal flow region at low frequencies, with no impact of neutralization on the slopes of G' and G" (**Table S8**).

One exception is the P(LMA-*co*-MAA) copolymer with 5 mol% total MAA and 5 mol% ion content (e.g., P(LMA_{95}-*co*-MAA_5^{Na})); in which all MAA repeat units are assumed to be fully neutralized. This polymer exhibited a plateau region at intermediate frequencies (**Figure 3a)** that may be due to the formation of a stable physical gel through the ion aggregates.[81] By contrast, partially neutralized samples that contain un-neutralized carboxylic acid groups on MAA could undergo hydrogen bonding and may have additional mechanisms for ion dynamics such as ion hopping[82-84] or destabilization of ionic aggregates[60, 71, 85] leading to a more dynamic network.

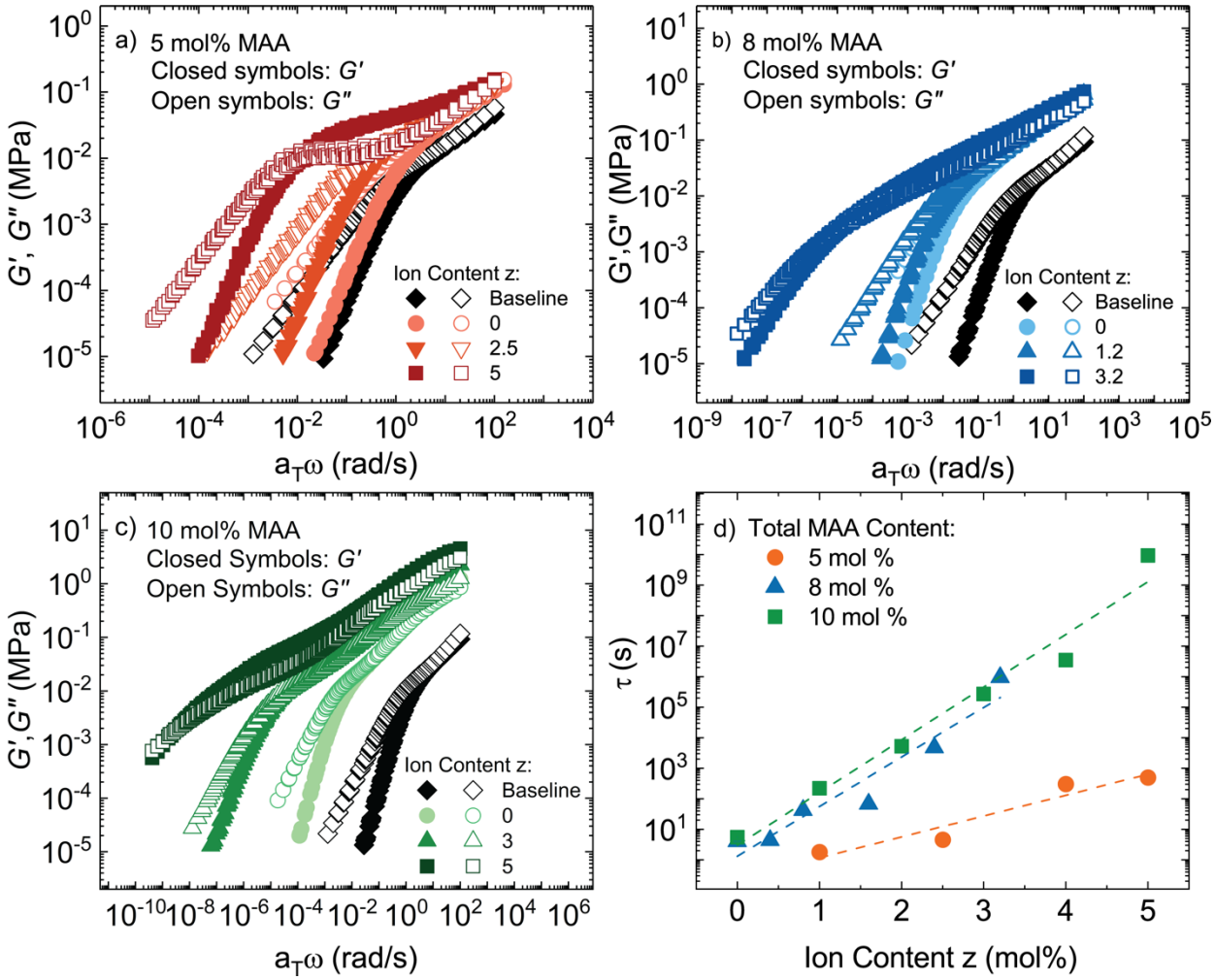

Figure 3. Storage (G', closed symbols) and loss (G", open symbols) moduli as a function of frequency for P(LMA-*co*-MAA) copolymers of total MAA content in the polymer (both neutralized and unneutralized) of (a) 5, (b) 8, and (c) 10 mol%, and varying ion content z (mol% Na-neutralized MAA repeat units). The baseline polymers, P(LMA-*co*-*t*BMA), do not exhibit hydrogen bonding or ionic interactions, and are shown as black symbols in each panel. Data were shifted through TTS using shift factor a_T. Temperature dependence of a_T is shown in **Figure S2**, with reference temperature near 30 °C (WLF parameters, reference temperatures, and shift factors are provided in **Tables S3-S7**). In (d), the relaxation time τ quantified from the crossover of G' and G" is shown as a function of ion content for each series, which is also the dynamic bond lifetime (τ_b) of the ion-containing or hydrogen bonding polymers. Error on τ was quantified to be smaller than the data points (see discussion of error analysis in the *Supporting Information*). Dashed lines represent linear fits to τ vs. ion content on a log-linear plot.

The crossover frequency (ω_{cr}) where $G' = G''$ can be used to measure the relaxation time of the polymer ($\tau = 2\pi/\omega_{cr}$), which is also the dynamic bond lifetime of the ion-containing or

hydrogen bonding polymers (τ_b).[79, 80, 86] τ_b is the characteristic time scale for the dissociation and association of the dynamic bonds responsible for the network mobility, which provides crucial insight into the dynamic behavior of the material.[87] It is worth noting that the dynamic bonds will break and reform many times before finally separating, thus τ measured from ω_{cr} should be considered as an effective bond lifetime which is greater than bare bond lifetime.[86] For each series of fixed total MAA content in the copolymer (5, 8 or 10 mol%), τ increased significantly with increasing ion content (**Figure 3d**). For polymers of similar ion content, increasing the total MAA content of the polymer also increased τ (**Figure 3d**), due to the increased presence of non-neutralized acid groups which can undergo hydrogen bonding that induce slower chain dynamics.

Arrhenius analysis was conducted on the temperature-dependence of the relaxation time for each neutralized P(LMA-*co*-MAA) copolymer with ion content z (e.g., P($LMA_{100-y-z}$-*co*-MAA_y-*co*-MAA_z^{Na}):[70, 80, 85]

$$\tau = A_o \exp\left(\frac{E_a}{RT}\right) \quad \text{(eq. 4)}$$

where A_o is the prefactor, E_a is the activation energy, R is the gas constant and T is the temperature. E_a was quantified from the slope when $\ln \tau$ was plotted as a function of $1/T$ (**Figure 4a**). Through this analysis, an activation energy was quantified, providing information on the energetics of the midblock dynamics as a function of MAA and ion content. E_a did not vary significantly with either ion or total MAA content (**Figure 4b.**). Prior literature reports have also demonstrated systems containing Na^+ ions in which E_a does not vary with ion content, which differs from the increasing trend in E_a with ion content that has been observed in other ion systems.[70, 80, 84] One possible explanation for this is that Na^+ has relatively higher mobility, faster diffusion, and shorter multiplet lifetimes than other cations.[70, 71, 80] Previously, it has been discussed that the time scales of chain diffusion is governed by that of ion hopping.[70, 88, 89] The invariance of E_a with ion content may

indicate the energy barrier that must be overcome for ion hopping is unaffected by the amount of ions and their aggregates in the system. Additionally, the values of E_a obtained here are similar in magnitude to what has been previously observed for ionic aggregates,[70, 80, 90] but slightly higher than that of other systems employing sodium ions specifically.[80, 82, 84, 91]

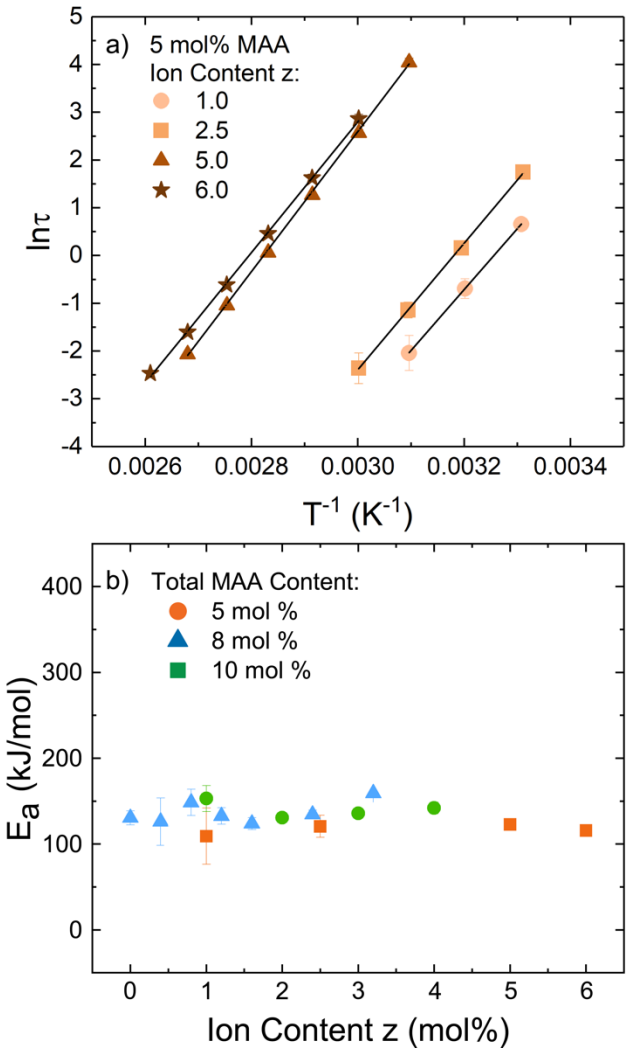

Figure 4. (a) Arrhenius plot of $\ln \tau$ vs. $1/T$ for P(LMA$_{95}$-*co*-MAA$_{5-z}$-*co*-MAA$_z^{Na}$) copolymers with varying ion content z (mol% Na-neutralized MAA repeat units). Lines indicate best fits of eq. 4 to the data. Error bars reflect measurement error based on instrument resolution and are sometimes smaller than data points (discussed in *Supporting Information*). (b) E_a vs. ion content z for neutralized P(LMA-*co*-MAA) copolymers of differing total MAA content. Error bars reflect standard error from linear fits and are sometimes smaller than the data points (discussed in the *Supporting Information*).

It is worth noting that trends in τ and E_a discussed here could in theory be impacted by variations in the ionic aggregate structure and size. Wide-angle X-ray scattering experiments were conducted on the P(LMA-*co*-MAA) copolymers and are shown in Figure S7, with additional details provided in the *Supporting Information* on the data collection and analysis. An estimation of the ionic aggregate size, provided through the domain spacing d ($d = 2\pi/q^*$, where q^* is the magnture of the scattering vector at the peak maximum) showed that the ionic aggregate size did not change significantly with variations in either acid or ion content.

Presence of Ionic Interactions Improves Mechanical Properties of PMMA-*b*-P(LMA-*co*-MAA)-*b*-PMMA Triblock Copolymers

Mechanical properties of ionic PMMA-*b*-P(LMA-*co*-MAA)-*b*-PMMA triblock copolymers were investigated by tensile testing (**Figure 5**, **Table S11**). Prior to hydrolysis and neutralization, the baseline PMMA-*co*-P(LMA-*co*-*t*BMA)-*co*-PMMA triblock copolymers exhibited both low tensile strength and strain at break, attributed to lack of entanglements in the midblock.[24] Upon hydrolysis and neutralization, which induce hydrogen bonding interactions (due to presence of un-neutralized MAA groups) and ionic interactions (due to presence of Na-neutralized MAA groups), PMMA-*b*-P(LMA-*co*-MAA)-*b*-PMMA triblock copolymers showed drastic changes in the stress-strain curves, with higher tensile strength and, in some cases, higher strain at break as compared to the baseline triblock copolymers.

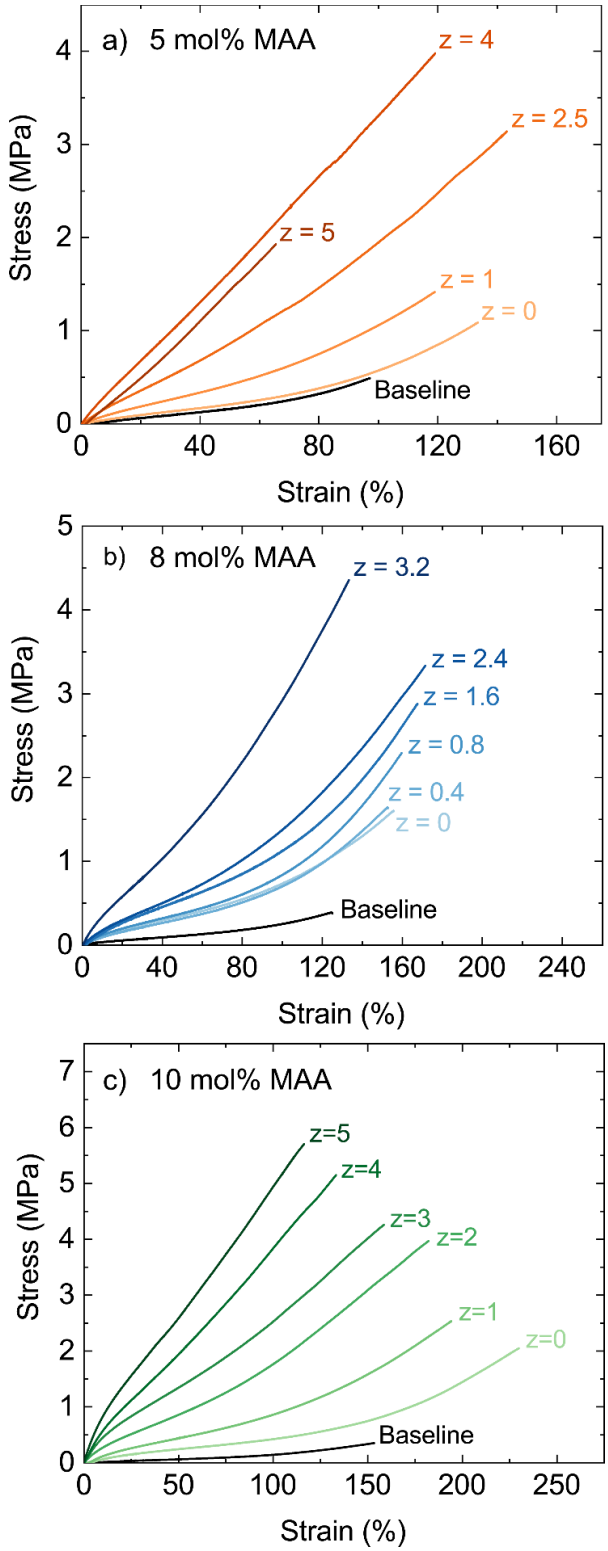

Figure 5. Tensile stress-strain curves for PMMA-*b*-P(LMA-*co*-MAA)-*b*-PMMA triblock copolymers of total MAA content in the midlock (both neutralized and un-neutralized) of (a) 5, (b) 8, and (c) 10 mol%, and varying ion content z (mol% Na-neutralized MAA repeat units in the

midblock). The baseline polymers, PMMA-*co*-P(LMA-*co*-*t*BMA)-*co*-PMMA, do not exhibit hydrogen bonding or ionic interactions, and are shown as black curves in each panel.

To quantify the impact of hydrogen bonding and ionic interactions on tensile properties we defined factors of enhancement ($F_{tensile\ strength}$ and $F_{strain\ at\ break}$) by dividing the tensile strength and strain at break of neutralized PMMA-*b*-P(LMA-*co*-MAA)-*b*-PMMA triblock copolymers by that of their precursor (PMMA-*b*-P(LMA-*co*-tBMA)-*b*-PMMA) (e.g. the "baseline polymer", that obtained prior to hydrolysis and neutralization), as described in **Table S11** and **eqs. S25 and S26**. We will first discuss the behavior of PMMA-*b*-P(LMA-*co*-MAA)-*b*-PMMA triblock copolymers prior to neutralization, and then discuss the impact of neutralization of the acid groups.

Incorporation of acidic MAA groups in the polymer (through hydrolysis of the midblock) can enable formation of a dynamic network through hydrogen bonding. For un-neutralized PMMA-*b*-P(LMA-*co*-MAA)-*b*-PMMA triblock copolymers, $F_{tensile\ strength}$ was in the range of 2.4 – 5.8 (a factor of 2 – 6 improvement as compared to the baseline polymer) and $F_{strain\ at\ break}$ was in the range of 1.2 – 1.5 (20 – 50% improvement as compared to the baseline polymer). As the total mol% MAA in the midblock increased, $F_{tensile\ strength}$ increased (**Table S11)**, which we propose is indicative of the effective transient crosslink density of the network (due to hydrogen bonding) increasing with increasing MAA content. Meanwhile, the total mol% MAA in the midblock did not affect $F_{strain\ at\ break}$.

Neutralization of acid groups can induce the formation of an ionic network in the polymer. Increasing the ion content (z) of the midblock drastically increased the triblock copolymer tensile strength (**Figure S8**). $F_{tensile\ strength}$ was as high as 17, indicating a factor of 17 improvement in tensile strength for the ionic triblock copolymers as compared to the baseline polymer. Prior literature studies have demonstrated an increase in tensile strength in ionic networks due to formation of ionic clusters that can act not only as transient crosslinkers but also as reinforcing

fillers.[60, 71, 85, 92, 93] Varying the ion content of the midblock brought about more modest changes in the strain at break of the triblock copolymer, with a maximum in the strain break observed at an intermediate ion content for each series of differing total mol% MAA (**Figure S8**). This could be understood by first considering that addition of ion content provides ionic interactions that act as dynamic crosslinks that enhance stress dissipation through the material, resulting in increased strain at break.[71, 94, 95] However, further addition of ions then causes reduction of chain mobility as the chains interact more strongly. As this continues, the polymer chains become increasingly arrested near the ionic aggregates, reducing stress dissipation and leading to reduction in strain at break at higher ion content.

We propose that enhancements observed in the triblock copolymer mechanical properties are governed by midblock bond dynamics. This system contains both hydrogen bonds and ionic bonds that can simultaneously act as transient crosslinkers in the matrix (midblock) phase of the PMMA-*b*-P(LMA-*co*-MAA)-*b*-PMMA triblock copolymers. The key element of both of these interactions is that they can rapidly associate and dissociate, allowing for additional mechanisms of energy dissipation and enhanced mechanical properties.[71, 94, 95] In order to investigate relationships between the midblock chain dynamics and triblock copolymer mechanical properties, we plotted $F_{tensile\ strength}$ and $F_{strain\ at\ break}$ as a function of the logarithm of the midblock relaxation time (log τ) measured through rheology, which is also a measure of the dynamic bond lifetime (τ_b) for polymers containing dynamic bonds (**Figure 6**). Importantly, $F_{tensile\ strength}$ and $F_{strain\ at\ break}$ of triblock copolymers of differing total acid (MAA) content and ion content (z) collapsed onto master curves when plotted vs. log τ, but not when plotted vs. ion content or acid content.

$F_{tensile\ strength}$ increased linearly with log τ. A number of factors may explain this relationship. Increasing the number of dynamic bonds, tuned through the acid and ion content of the polymer, is expected to increase the effective crosslink density of the transient network and enhance the tensile strength. Similarly, the greater the number of dynamic bonds, the more slowly the material is anticipated to relax, and thus exhibit a longer relaxation time.

$F_{strain\ at\ break}$ showed relatively consistent enhancement at short relaxation times (< 10^3 s), then decreased at longer relaxation times. At short relaxation times, the dynamic bonds can associate and dissociate fast enough to dissipate energy through the material and allow higher extensibility but still reduce stress concentrations that lead to material failure .[24, 26, 96] However, increasing amounts of ions added to the system leads to longer relaxation times, likely reflecting limitations in chain mobility resulting in poor energy dissipation. Thus, at long relaxation times, though the tensile strength improved significantly, the strain at break decreased.

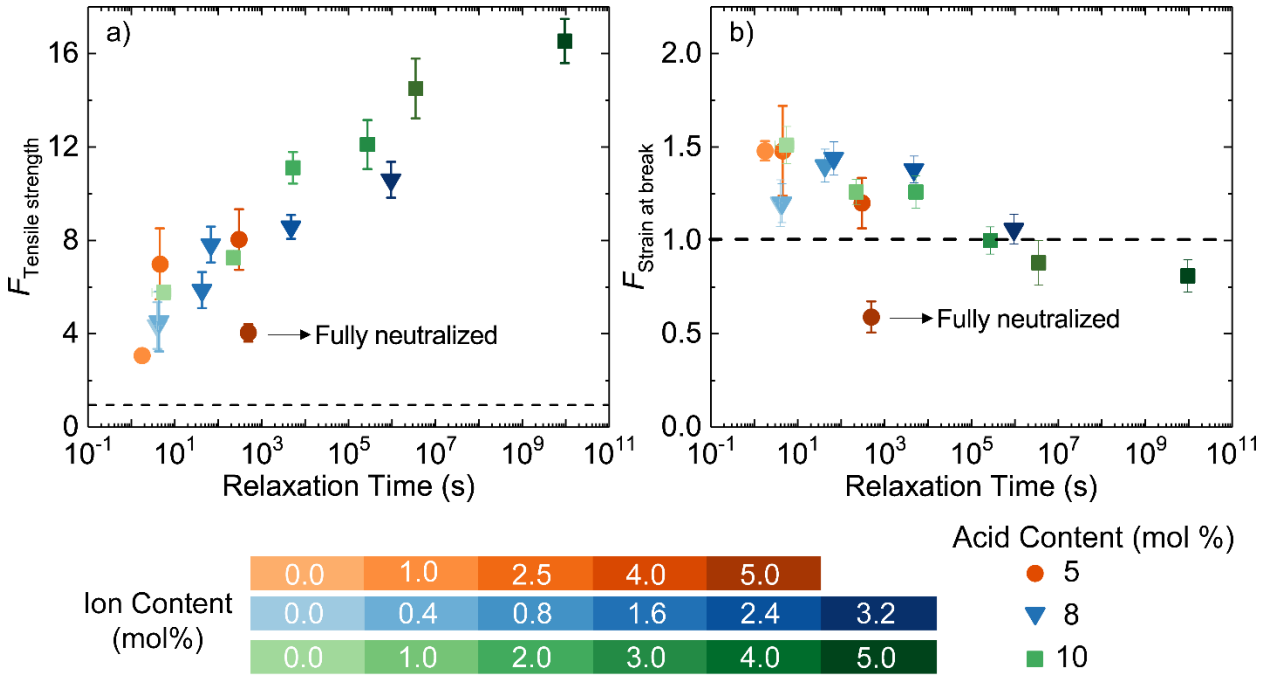

Figure 6. Factors of enhancement, (a) $F_{tensile\ strength}$ and (b) $F_{strain\ at\ break}$, for PMMA-*b*-P(LMA-*co*-MAA)-*b*-PMMA triblock copolymers of total MAA content in the midlock (both neutralized and un-neutralized) of 5, 8, and 10 mol%, and varying ion content z (mol% Na-neutralized MAA repeat units in the midblock). The ion content z is indicated by the data point

shading as shown in the legend. The dashed lines indicate the factor of enhancement of 1 for the baseline polymer, PMMA-*co*-P(LMA-*co*-*t*BMA)-*co*-PMMA. The fully neutralized polymer (indicated by an arrow) contained only neutralized MAA groups. In some cases, the time for completion of the tensile test was greater than the midblock relaxation time (Table S12).

$F_{tensile\ strength}$ and $F_{strain\ at\ break}$ of PMMA-*b*-P(LMA$_{95}$-*co*-MAA$_5^{Na}$)-*b*-PMMA are lower than that of other samples with similar relaxation times (see outlier data points in Figure 6). This behavior is attributed to the complete neutralization of this material. Recall from previous discussion that the midblock P(LMA$_{95}$-co-MAA$_5^{Na}$) showed a plateau region of G' at intermediate frequencies, indicating a formation of a physical network due to presence of large ion aggregates. These large ion aggregates are likely more stable than smaller ion clusters or multiplets, and thus exhibit slower dynamics.[60, 85, 97] Additionally, other studies have proposed and investigated an "ion hopping" mechanism where ions are able to effectively migrate from one ionic aggregate structure to another.[33, 70, 84, 85] It is believed that the rate at which ions are able to migrate between aggregates can cause significant impacts on the stress relaxation and overall chain mobility, since multiple ion hopping events may be required for significant or longer distance chain motion.[25, 82, 84] It has been demonstrated that excess acid can act as plasticizer that can enhance ion mobility and destabilize ionic aggregates.[71, 97, 98] We therefore propose that the lack of excess acid in the fully neutralized (PMMA-*b*-P(LMA$_{95}$-*co*-MAA$_5^{Na}$)-*b*-PMMA) results in a slower ion hoping rate due to more stable ionic aggregates, leading to reduction in tensile properties.

Conclusions

Ionic bonds were introduced into fatty acid-derived thermoplastic elastomers (TPEs) to enhance their mechanical properties. The comonomer methacrylic acid was neutralized with NaOH to incorporate ionic interactions into polymers. The effects of acid content and ion content on the rheological properties of the midblock and the mechanical properties of the triblock copolymers were evaluated. The midblock relaxation time increased with both increasing ion content and acid content and an Arrhenius analysis of the relaxation time, unexpectedly revealing the activation energy did not vary with acid and ion content. Mechanical properties of the triblock copolymer samples were improved significantly by the incorporation of ionic interactions. The mechanical property factors of enhancement were shown to correlate well with the relaxation time of the midblock, with the data collapsing onto master curves for all acid and ion contents for both strain at break and tensile strength. The enhancement of tensile strength increased linearly with the logarithm of relaxation time and showed as high as a 17-fold improvement compared to the baseline material without ionic interactions and hydrogen bonding, and 16-fold improvement without significant loss in extensibility. Meanwhile, the strain at break exhibited moderate enhancement at short relaxation times before decreasing at longer relaxation times to values less than that of the baseline material.

This collapse of the tensile data onto master curves as a function of the midblock relaxation time, but not ion content or acid content, supports our hypothesis that the midblock chain dynamics are a governing factor in the mechanical property enhancements in these materials. Additionally, the only sample with fully neutralized acid groups was also the only one that deviated significantly from the master curves. This suggests the unneutralized acid groups may enhance ion mobility and destabilize ionic aggregates through a plasticization effect.

Supporting information: Polymer characteristics (Tables S1 – S2, Figure S1); horizontal shift factors (Figure S2 and Tables S4 – S7); Williams-Landel-Ferry equation (eq. S1) parameters (Table S3); terminal slopes of G' and G" vs. ω (Table S8); G' and G' vs. ω for samples with 0% ion content (Figure S3); error analysis for relaxation time (Tables S9 – S10, Figures S4 – S5); error analysis for activation energy (Figure S6); mechanical properties (Table S11, Table S12); wide-angle X-ray scattering data (Figure S7); factors of enhancement in tensile strength and strain at break as functions of ion content of midblock (Figure S8). (PDF)

Acknowledgements

The authors thank Dr. Brian Rohde for assistance and discussion of FTIR experiments and Dr. Shu Wang for helpful discussions about RAFT polymerization. The authors appreciate the assistance of Dr. Charles Anderson and Dr. Scott Smith for access and training in the University of Houston Department of Chemistry Nuclear Magnetic Resonance Facility. This material is based upon work supported by the National Science Foundation under Grant No. DMR-1906009. Additional support was provided by the Welch Foundation under Grant No. E-2160.

References

(1) Bonart, R. Thermoplastic elastomers. *Polymer* **1979**, *20* (11), 1389-1403. DOI: https://doi.org/10.1016/0032-3861(79)90280-5.

(2) Shanks, R. A. General purpose elastomers: structure, chemistry, physics and performance. In *Advances in elastomers I*, Springer, 2013; pp 11-45.

(3) Wang, W.; Lu, W.; Goodwin, A.; Wang, H.; Yin, P.; Kang, N.-G.; Hong, K.; Mays, J. W. Recent advances in thermoplastic elastomers from living polymerizations: Macromolecular architectures and supramolecular chemistry. *Progress in Polymer Science* **2019**, *95*, 1-31. DOI: https://doi.org/10.1016/j.progpolymsci.2019.04.002.

(4) Salman Amin, M. A. Thermoplastic Elastomeric (TPE) Materials and Their Use in Outdoor Electrical Insulation. *Reviews on Advanced Materials Science* **2011**, *29*, 15-30.

(5) Fiorentino, G.; Ripa, M.; Ulgiati, S. Chemicals from biomass: technological versus environmental feasibility. A review. *Biofuels, Bioproducts and Biorefining* **2016**, *11* (1), 195-214. DOI: 10.1002/bbb.1729.

(6) Getzler, Y.; Mathers, R. T. Sustainable Polymers: Our Evolving Understanding. *Acc Chem Res* **2022**, *55* (14), 1869-1878. DOI: 10.1021/acs.accounts.2c00194 From NLM Medline.

(7) Mohanty, A. K.; Wu, F.; Mincheva, R.; Hakkarainen, M.; Raquez, J.-M.; Mielewski, D. F.; Narayan, R.; Netravali, A. N.; Misra, M. Sustainable polymers. *Nature Reviews Methods Primers* **2022**, *2* (1), 46. DOI: 10.1038/s43586-022-00124-8.

(8) Comí, M.; Lligadas, G.; Ronda, J. C.; Galià, M.; Cádiz, V. Adaptive bio-based polyurethane elastomers engineered by ionic hydrogen bonding interactions. *European Polymer Journal* **2017**, *91*, 408-419. DOI: https://doi.org/10.1016/j.eurpolymj.2017.04.026.

(9) Lee, S.; Yuk, J. S.; Park, H.; Kim, Y.-W.; Shin, J. Multiblock Thermoplastic Elastomers Derived from Biodiesel, Poly(propylene glycol), and l-Lactide. *ACS Sustainable Chemistry & Engineering* **2017**, *5* (9), 8148-8160. DOI: 10.1021/acssuschemeng.7b01801.

(10) Wang, S.; Vajjala Kesava, S.; Gomez, E. D.; Robertson, M. L. Sustainable Thermoplastic Elastomers Derived from Fatty Acids. *Macromolecules* **2013**, *46* (18), 7202-7212. DOI: 10.1021/ma4011846.

(11) Frick, E. M.; Zalusky, A. S.; Hillmyer, M. A. Characterization of Polylactide-b-polyisoprene-b-polylactide Thermoplastic Elastomers. *Biomacromolecules* **2003**, *4* (2), 216-223.

(12) Zhou, C.; Wei, Z. Y.; Lei, X. F.; Li, Y. Fully biobased thermoplastic elastomers: synthesis and characterization of poly(L-lactide)-b-polymyrcene-b-poly(L-lactide) triblock copolymers. *Rsc Advances* **2016**, *6* (68), 63508-63514, Article. DOI: 10.1039/c6ra08689f.

(13) Fang, C.; Wang, X.; Chen, X.; Wang, Z. Mild synthesis of environment-friendly thermoplastic triblock copolymer elastomers through combination of ring-opening and RAFT polymerization. *Polymer Chemistry* **2019**, *10* (26), 3610-3620, 10.1039/C9PY00654K. DOI: 10.1039/C9PY00654K.

(14) Nasiri, M.; Saxon, D. J.; Reineke, T. M. Enhanced Mechanical and Adhesion Properties in Sustainable Triblock Copolymers via Non-covalent Interactions. *Macromolecules* **2018**, *51* (7), 2456-2465. DOI: 10.1021/acs.macromol.7b02248.

(15) Ganewatta, M. S.; Ding, W.; Rahman, M. A.; Yuan, L.; Wang, Z.; Hamidi, N.; Robertson, M. L.; Tang, C. Biobased Plastics and Elastomers from Renewable Rosin via "Living" Ring-Opening Metathesis Polymerization. *Macromolecules* **2016**, *49* (19), 7155-7164. DOI: 10.1021/acs.macromol.6b01496.

(16) Ding, W.; Wang, S.; Yao, K.; Ganewatta, M. S.; Tang, C.; Robertson, M. L. Physical Behavior of Triblock Copolymer Thermoplastic Elastomers Containing Sustainable Rosin-Derived Polymethacrylate End Blocks. *ACS Sustainable Chemistry & Engineering* **2017**, *5* (12), 11470-11480. DOI: 10.1021/acssuschemeng.7b02676.

(17) Chen, X.; Zhou, Z.; Zhang, H.; Mao, Y.; Luo, Z.; Li, X.; Sha, Y. Sustainable Thermoplastic Elastomers Derived from Lignin Bio-Oils via an ABA Triblock Copolymer Strategy. *Macromolecular Chemistry and Physics* **2021**, *222* (11), 2100055. DOI: https://doi.org/10.1002/macp.202100055 (acccessed 2023/12/15).
(18) Wan, Y.; He, J.; Zhang, Y.; Chen, E. Y. X. One-Step Synthesis of Lignin-Based Triblock Copolymers as High-Temperature and UV-Blocking Thermoplastic Elastomers. *Angewandte Chemie* **2022**, *134* (8), e202114946. DOI: https://doi.org/10.1002/ange.202114946 (acccessed 2023/12/15).
(19) Bolton, J. M.; Hillmyer, M. A.; Hoye, T. R. Sustainable Thermoplastic Elastomers from Terpene-Derived Monomers. *ACS Macro Letters* **2014**, *3* (8), 717-720. DOI: 10.1021/mz500339h.
(20) Sahu, P.; Bhowmick, A. K.; Gergely, K. Terpene Based Elastomers: Synthesis, Properties, and Applications. *Processes* **2020**, *8* (5), 553. DOI: https://doi.org/10.3390/pr8050553 Publicly Available Content Database; SciTech Premium Collection.
(21) Winnacker, M. Pinenes: Abundant and Renewable Building Blocks for a Variety of Sustainable Polymers. *Angewandte Chemie International Edition* **2018**, *57* (44), 14362-14371. DOI: https://doi.org/10.1002/anie.201804009 (acccessed 2023/12/15).
(22) Whelan, D. Thermoplastic Elastomers. In *Brydson's Plastics Materials*, 2017; pp 653-703.
(23) Holden, G. 6 - Thermoplastic Elastomers. In *Applied Plastics Engineering Handbook*, Kutz, M. Ed.; William Andrew Publishing, 2011; pp 77-91.
(24) Tong, J.-D.; Jerôme, R. Dependence of the Ultimate Tensile Strength of Thermoplastic Elastomers of the Triblock Type on the Molecular Weight between Chain Entanglements of the Central Block. *Macromolecules* **2000**, *33* (5), 1479-1481. DOI: 10.1021/ma990404f.
(25) Ling, G. H.; Wang, Y.; Weiss, R. A. Linear Viscoelastic and Uniaxial Extensional Rheology of Alkali Metal Neutralized Sulfonated Oligostyrene Ionomer Melts. *Macromolecules* **2011**, *45* (1), 481-490. DOI: 10.1021/ma201854w.
(26) Baeurle, S. A.; Hotta, A.; Gusev, A. A. A new semi-phenomenological approach to predict the stress relaxation behavior of thermoplastic elastomers. *Polymer* **2005**, *46* (12), 4344-4354. DOI: https://doi.org/10.1016/j.polymer.2004.07.034.
(27) Wang, S.; Ding, W.; Yang, G.; Robertson, M. L. Biorenewable Thermoplastic Elastomeric Triblock Copolymers Containing Salicylic Acid-Derived End-Blocks and a Fatty Acid-Derived Midblock. *Macromolecular Chemistry and Physics* **2016**, *217* (2), 292-303. DOI: 10.1002/macp.201500274.
(28) Wang, Z.; Yuan, L.; Trenor, N. M.; Vlaminck, L.; Billiet, S.; Sarkar, A.; Du Prez, F. E.; Stefik, M.; Tang, C. Sustainable thermoplastic elastomers derived from plant oil and their “click-coupling” via TAD chemistry. *Green Chemistry* **2015**, *17* (7), 3806-3818.
(29) Wang, Z.; Yuan, L.; Tang, C. Sustainable Elastomers from Renewable Biomass. *Acc Chem Res* **2017**, *50* (7), 1762-1773. DOI: 10.1021/acs.accounts.7b00209 From NLM PubMed-not-MEDLINE.
(30) Zhao, W.; Li, C.; Yang, X.; He, J.; Pang, X.; Zhang, Y.; Men, Y.; Chen, X. One-Pot Synthesis of Supertough, Sustainable Polyester Thermoplastic Elastomers Using Block-Like, Gradient Copolymer as Soft Midblock. *CCS Chemistry* **2022**, *4* (4), 1263-1272.
(31) Zhu, Y.; Romain, C.; Williams, C. K. Sustainable polymers from renewable resources. *Nature* **2016**, *540* (7633), 354-362. DOI: 10.1038/nature21001 From NLM Medline.
(32) Huang, J.; Liu, W.; Qiu, X. High Performance Thermoplastic Elastomers with Biomass Lignin as Plastic Phase. *ACS Sustainable Chemistry & Engineering* **2019**, *7* (7), 6550-6560. DOI: 10.1021/acssuschemeng.8b04936.
(33) Utrera-Barrios, S.; Ricciardi, O.; González, S.; Verdejo, R.; López-Manchado, M. Á.; Hernández Santana, M. Development of Sustainable, Mechanically Strong, and Self-Healing Bio-Thermoplastic Elastomers Reinforced with Alginates. In *Polymers*, 2022; Vol. 14.
(34) Nurhamiyah, Y.; Yoon, S.; Chen, B. Wholly Biobased Polyamide Thermoplastic Elastomer-Cellulose Nanocomposites. *Macromolecular Materials and Engineering* **2022**, *307* (6), 2200120. DOI: https://doi.org/10.1002/mame.202200120 (acccessed 2023/09/14).

(35) Ortiz-Serna, P.; Carsí, M.; Culebras, M.; Collins, M.; Sanchis, M. Exploring the role of lignin structure in molecular dynamics of lignin/bio-derived thermoplastic elastomer polyurethane blends. *International journal of biological macromolecules* **2020**, *158*, 1369-1379.
(36) Gregory, G. L.; Williams, C. K. Exploiting Sodium Coordination in Alternating Monomer Sequences to Toughen Degradable Block Polyester Thermoplastic Elastomers. *Macromolecules* **2022**, *55* (6), 2290-2299. DOI: 10.1021/acs.macromol.2c00068.
(37) Miwa, Y.; Kurachi, J.; Kohbara, Y.; Kutsumizu, S. Dynamic ionic crosslinks enable high strength and ultrastretchability in a single elastomer. *Communications Chemistry* **2018**, *1* (1). DOI: 10.1038/s42004-017-0004-9.
(38) Jiang, F.; Wang, Z.; Zhang, X.; Henderson, D.; Hwang, W.; Briber, R. M.; Wang, H. Synergistically Tailoring Mechanical and Optical Properties of Diblock Copolymer Thermoplastic Elastomers via Lanthanide Coordination. *Chemistry of Materials* **2022**, *34* (4), 1578-1589. DOI: 10.1021/acs.chemmater.1c03264.
(39) Nurhamiyah, Y.; Amir, A.; Finnegan, M.; Themistou, E.; Edirisinghe, M.; Chen, B. Wholly Biobased, Highly Stretchable, Hydrophobic, and Self-healing Thermoplastic Elastomer. *ACS Applied Materials & Interfaces* **2021**, *13* (5), 6720-6730. DOI: 10.1021/acsami.0c23155.
(40) Herbst, F.; Dohler, D.; Michael, P.; Binder, W. H. Self-healing polymers via supramolecular forces. *Macromol Rapid Commun* **2013**, *34* (3), 203-220. DOI: 10.1002/marc.201200675 From NLM Medline.
(41) Poon, K. C.; Gregory, G. L.; Sulley, G. S.; Vidal, F.; Williams, C. K. Toughening CO2-Derived Copolymer Elastomers Through Ionomer Networking. *Advanced Materials* **2023**, *35* (36), 2302825. DOI: https://doi.org/10.1002/adma.202302825 (acccessed 2024/07/25).
(42) Liu, B.; Chen, X.; Spiering, G. A.; Moore, R. B.; Long, T. E. Quadruple hydrogen bond-containing a-ab-a triblock copolymers: Probing the influence of hydrogen bonding in the central block. *Molecules* **2021**, *26* (15), 4705.
(43) Wang, W.; Zhang, J.; Jiang, F.; Wang, X.; Wang, Z. Reprocessable Supramolecular Thermoplastic BAB-Type Triblock Copolymer Elastomers with Enhanced Tensile Strength and Toughness via Metal–Ligand Coordination. *ACS Applied Polymer Materials* **2019**, *1* (3), 571-583. DOI: 10.1021/acsapm.8b00277.
(44) Gregory, G. L.; Sulley, G. S.; Kimpel, J.; Łagodzińska, M.; Häfele, L.; Carrodeguas, L. P.; Williams, C. K. Block Poly(carbonate-ester) Ionomers as High-Performance and Recyclable Thermoplastic Elastomers. *Angewandte Chemie* **2022**, *134* (47), e202210748. DOI: https://doi.org/10.1002/ange.202210748 (acccessed 2023/09/15).
(45) Jiang, F.; Fang, C.; Zhang, J.; Wang, W.; Wang, Z. Triblock Copolymer Elastomers with Enhanced Mechanical Properties Synthesized by RAFT Polymerization and Subsequent Quaternization through Incorporation of a Comonomer with Imidazole Groups of about 2.0 Mass Percentage. *Macromolecules* **2017**, *50* (16), 6218-6226. DOI: 10.1021/acs.macromol.7b01414.
(46) Jiang, F.; Zhang, X.; Hwang, W.; Briber, R. M.; Fang, Y.; Wang, H. Supramolecular luminescent triblock copolymer thermoplastic elastomer via metal-ligand coordination. *Polymer Testing* **2019**, *78*. DOI: 10.1016/j.polymertesting.2019.105956.
(47) Voorhaar, L.; Diaz, M. M.; Leroux, F.; Rogers, S.; Abakumov, A. M.; Van Tendeloo, G.; Van Assche, G.; Van Mele, B.; Hoogenboom, R. Supramolecular thermoplastics and thermoplastic elastomer materials with self-healing ability based on oligomeric charged triblock copolymers. *NPG Asia Materials* **2017**, *9* (5), e385-e385. DOI: 10.1038/am.2017.63.
(48) Ding, W.; Robertson, M. L. Sustainable thermoplastic elastomers with a transient network. *European Polymer Journal* **2019**, *113*, 411-423. DOI: https://doi.org/10.1016/j.eurpolymj.2019.01.010.
(49) Hayashi, M.; Matsushima, S.; Noro, A.; Matsushita, Y. Mechanical Property Enhancement of ABA Block Copolymer-Based Elastomers by Incorporating Transient Cross-Links into Soft Middle Block. *Macromolecules* **2015**, *48* (2), 421-431. DOI: 10.1021/ma502239w.

(50) Hayashi, M.; Noro, A.; Matsushita, Y. Highly Extensible Supramolecular Elastomers with Large Stress Generation Capability Originating from Multiple Hydrogen Bonds on the Long Soft Network Strands. *Macromol Rapid Commun* **2016**, *37* (8), 678-684. DOI: 10.1002/marc.201500663 From NLM.
(51) Yang, J.-X.; Long, Y.-Y.; Pan, L.; Men, Y.-F.; Li, Y.-S. Spontaneously Healable Thermoplastic Elastomers Achieved through One-Pot Living Ring-Opening Metathesis Copolymerization of Well-Designed Bulky Monomers. *ACS Applied Materials & Interfaces* **2016**, *8* (19), 12445-12455. DOI: 10.1021/acsami.6b02073.
(52) Mather, B. D.; Baker, M. B.; Beyer, F. L.; Berg, M. A.; Green, M. D.; Long, T. E. Supramolecular triblock copolymers containing complementary nucleobase molecular recognition. *Macromolecules* **2007**, *40* (19), 6834-6845.
(53) Söntjens, S. H.; Renken, R. A.; van Gemert, G. M.; Engels, T. A.; Bosman, A. W.; Janssen, H. M.; Govaert, L. E.; Baaijens, F. P. Thermoplastic elastomers based on strong and well-defined hydrogen-bonding interactions. *Macromolecules* **2008**, *41* (15), 5703-5708.
(54) Zhang, K.; Aiba, M.; Fahs, G. B.; Hudson, A. G.; Chiang, W. D.; Moore, R. B.; Ueda, M.; Long, T. E. Nucleobase-functionalized acrylic ABA triblock copolymers and supramolecular blends. *Polymer Chemistry* **2015**, *6* (13), 2434-2444. DOI: 10.1039/c4py01798f.
(55) Appel, W. P. J.; Portale, G.; Wisse, E.; Dankers, P. Y. W.; Meijer, E. W. Aggregation of Ureido-Pyrimidinone Supramolecular Thermoplastic Elastomers into Nanofibers: A Kinetic Analysis. *Macromolecules* **2011**, *44* (17), 6776-6784. DOI: 10.1021/ma201303s.
(56) Wittenberg, E.; Meyer, A.; Eggers, S.; Abetz, V. Hydrogen bonding and thermoplastic elastomers - a nice couple with temperature-adjustable mechanical properties. *Soft Matter* **2018**, *14* (14), 2701-2711. DOI: 10.1039/C8SM00296G.
(57) Wang, Q.; He, Y.; Li, Q.; Wu, C. SBS Thermoplastic Elastomer Based on Dynamic Metal-Ligand Bond: Structure, Mechanical Properties, and Shape Memory Behavior. *Macromolecular Materials and Engineering* **2021**, *306* (5). DOI: 10.1002/mame.202000737.
(58) Yu, K.; Xin, A.; Feng, Z.; Lee, K. H.; Wang, Q. Mechanics of self-healing thermoplastic elastomers. *Journal of the Mechanics and Physics of Solids* **2020**, *137*, 103831. DOI: https://doi.org/10.1016/j.jmps.2019.103831.
(59) Burattini, S.; Colquhoun, H. M.; Fox, J. D.; Friedmann, D.; Greenland, B. W.; Harris, P. J. F.; Hayes, W.; Mackay, M. E.; Rowan, S. J. A self-repairing, supramolecular polymer system: healability as a consequence of donor–acceptor π–π stacking interactions. *Chemical Communications* **2009**, (44), 6717-6719, 10.1039/B910648K. DOI: 10.1039/B910648K.
(60) Prince Antony, S. K. D. Ionic Thermoplastic Elastomers: A Review. *Journal of Macromolecular Science - Polymer Reviews* **2001**, 41-77.
(61) Thomas Kurian, D. K., P. P. De, D. K. Tripathy, S. K. De. Plasticization of an ionic thermoplastic elastomer based on a zinc sulfonated ethylene-propylene-diene terpolymer of high ethylene content. *Polymer* **1995**, *37* (3).
(62) Kalista, S. J.; Pflug, J. R.; Varley, R. J. Effect of ionic content on ballistic self-healing in EMAA copolymers and ionomers. *Polymer Chemistry* **2013**, *4* (18). DOI: 10.1039/c3py00095h.
(63) Liu, X.; Zhao, R.-Y.; Zhao, T.-P.; Liu, C.-Y.; Yang, S.; Chen, E.-Q. An ABA triblock containing a central soft block of poly[2,5-di(n-hexogycarbonyl)styrene] and outer hard block of poly(4-vinylpyridine): synthesis, phase behavior and mechanical enhancement. *RSC Advances* **2014**, *4* (35), 18431-18441, 10.1039/C4RA01652A. DOI: 10.1039/C4RA01652A.
(64) Hayashi, M.; Noro, A.; Matsushita, Y. Highly Extensible Supramolecular Elastomers with Large Stress Generation Capability Originating from Multiple Hydrogen Bonds on the Long Soft Network Strands. *Macromolecular Rapid Communications* **2016**, *37* (8), 678-684. DOI: 10.1002/marc.201500663.
(65) Pan, G.-F.; Wang, Z.; Gong, X.-B.; Wang, Y.-F.; Ge, X.; Xing, R.-G. Self-healable recyclable thermoplastic polyurethane elastomers: Enabled by metal–ligand bonds between the cerium(III) triflate and phloretin. *Chemical Engineering Journal* **2022**, *446*, 137228. DOI: https://doi.org/10.1016/j.cej.2022.137228.

(66) Ding, W.; Hanson, J.; Burghardt, W. R.; López-Barrón, C. R.; Robertson, M. L. Shear Alignment Mechanisms of Close-Packed Spheres in a Bulk ABA Triblock Copolymer. *Macromolecules* **2022**, *55* (21), 9465-9477. DOI: 10.1021/acs.macromol.2c01245.
(67) Wang, S.; Xie, R.; Vajjala Kesava, S.; Gomez, E. D.; Cochran, E. W.; Robertson, M. L. Close-Packed Spherical Morphology in an ABA Triblock Copolymer Aligned with Large-Amplitude Oscillatory Shear. *Macromolecules* **2016**, *49* (13), 4875-4888. DOI: 10.1021/acs.macromol.6b00505.
(68) Chatterjee, D. P.; Mandal, B. M. Triblock Thermoplastic Elastomers with Poly(lauryl methacrylate) as the Center Block and Poly(methyl methacrylate) or Poly(tert-butyl methacrylate) as End Blocks. Morphology and Thermomechanical Properties. *Macromolecules* **2006**, *39* (26), 9192-9200. DOI: 10.1021/ma061391q.
(69) Sajjad, H.; Tolman, W. B.; Reineke, T. M. Block Copolymer Pressure-Sensitive Adhesives Derived from Fatty Acids and Triacetic Acid Lactone. *ACS Applied Polymer Materials* **2020**, *2* (7), 2719-2728. DOI: 10.1021/acsapm.0c00317.
(70) Neena K. Tierney, R. A. R. Ion Hopping in Ethylene-Methacrylic Acid Ionomer Melts as Probed by Rheometry and Cation Diffusion Measurements. *Macromolecules* **2001**, *35* (6).
(71) Eisenberg, M. N. a. A. Ion Clustering and Viscoelastic Relaxation in Styrene-Based Ionomers. III. Effect of Counterions, Carboxylic Groups, and Plasticizers. *Macromolecules* **1973**, *7* (1).
(72) Grady, B. P.; Goossens, J. G. P.; Wouters, M. E. L. Morphology of Zinc-Neutralized Maleated Ethylene−Propylene Copolymer Ionomers: Structure of Ionic Aggregates As Studied by X-ray Absorption Spectroscopy. *Macromolecules* **2004**, *37* (23), 8585-8591. DOI: 10.1021/ma048978u.
(73) Welty, A.; Ooi, S.; Grady, B. P. Effect of Water on Internal Aggregate Structure in Zinc-Neutralized Ionomers. *Macromolecules* **1999**, *32* (9), 2989-2995. DOI: 10.1021/ma981678q.
(74) Fragiadakis, D.; Dou, S.; Colby, R. H.; Runt, J. Molecular Mobility, Ion Mobility, and Mobile Ion Concentration in Poly(ethylene oxide)-Based Polyurethane Ionomers. *Macromolecules* **2008**, *41* (15), 5723-5728. DOI: 10.1021/ma800263b.
(75) Barner-Kowollik, C.; Buback, M.; Charleux, B.; Coote, M. L.; Drache, M.; Fukuda, T.; Goto, A.; Klumperman, B.; Lowe, A. B.; Mcleary, J. B.; et al. Mechanism and kinetics of dithiobenzoate-mediated RAFT polymerization. I. The current situation. *Journal of Polymer Science Part A: Polymer Chemistry* **2006**, *44* (20), 5809-5831. DOI: doi:10.1002/pola.21589.
(76) Chen, M.; Moad, G.; Rizzardo, E. Thiocarbonylthio end group removal from RAFT-synthesized polymers by a radical-induced process. *Journal of Polymer Science Part A: Polymer Chemistry* **2009**, *47* (23), 6704-6714. DOI: doi:10.1002/pola.23711.
(77) Hill, M. R.; Carmean, R. N.; Sumerlin, B. S. Expanding the Scope of RAFT Polymerization: Recent Advances and New Horizons. *Macromolecules* **2015**, *48* (16), 5459-5469. DOI: 10.1021/acs.macromol.5b00342.
(78) Herbst, F.; Seiffert, S.; Binder, W. H. Dynamic supramolecular poly(isobutylene)s for self-healing materials. *Polymer Chemistry* **2012**, *3* (11), 3084-3092, 10.1039/C2PY20265D. DOI: 10.1039/C2PY20265D.
(79) Serpe, M. J.; Craig, S. L. Physical Organic Chemistry of Supramolecular Polymers. *Langmuir* **2007**, *23* (4), 1626-1634. DOI: 10.1021/la0621416.
(80) Bose, R. K.; Hohlbein, N.; Garcia, S. J.; Schmidt, A. M.; Van Der Zwaag, S. Connecting supramolecular bond lifetime and network mobility for scratch healing in poly (butyl acrylate) ionomers containing sodium, zinc and cobalt. *Physical Chemistry Chemical Physics* **2015**, *17* (3), 1697-1704.
(81) Chen, Q.; Huang, C.; Weiss, R. A.; Colby, R. H. Viscoelasticity of Reversible Gelation for Ionomers. *Macromolecules* **2015**, *48* (4), 1221-1230. DOI: 10.1021/ma502280g.
(82) Tierney, N. K.; Register, R. A. Ion Hopping in Ethylene−Methacrylic Acid Ionomer Melts As Probed by Rheometry and Cation Diffusion Measurements. *Macromolecules* **2002**, *35* (6), 2358-2364. DOI: 10.1021/ma011775a.

(83) Hall, L. M.; Stevens, M. J.; Frischknecht, A. L. Dynamics of Model Ionomer Melts of Various Architectures. *Macromolecules* **2012**, *45* (19), 8097-8108. DOI: 10.1021/ma301308n.
(84) Vanhoorne, P.; Register, R. A. Low-Shear Melt Rheology of Partially-Neutralized Ethylene−Methacrylic Acid Ionomers. *Macromolecules* **1996**, *29* (2), 598-604. DOI: 10.1021/ma951143m.
(85) Hird, B.; Eisenberg, A. Sizes and stabilities of multiplets and clusters in carboxylated and sulfonated styrene ionomers. *Macromolecules* **1992**, *25* (24), 6466-6474.
(86) Feldman, K. E.; Kade, M. J.; Meijer, E. W.; Hawker, C. J.; Kramer, E. J. Model Transient Networks from Strongly Hydrogen-Bonded Polymers. *Macromolecules* **2009**, *42* (22), 9072-9081. DOI: 10.1021/ma901668w (acccessed 2013/07/20).
(87) Stukalin, E. B.; Cai, L.-H.; Kumar, N. A.; Leibler, L.; Rubinstein, M. Self-Healing of Unentangled Polymer Networks with Reversible Bonds. *Macromolecules* **2013**, *46* (18), 7525-7541. DOI: 10.1021/ma401111n.
(88) Orler, E. B.; Calhoun, B. H.; Moore, R. B. Crystallization Kinetics as a Probe of the Dynamic Network in Lightly Sulfonated Syndiotactic Polystyrene Ionomers. *Macromolecules* **1996**, *29* (18), 5965-5971. DOI: 10.1021/ma960003p.
(89) Tudryn, G. J.; O'Reilly, M. V.; Dou, S.; King, D. R.; Winey, K. I.; Runt, J.; Colby, R. H. Molecular Mobility and Cation Conduction in Polyether–Ester–Sulfonate Copolymer Ionomers. *Macromolecules* **2012**, *45* (9), 3962-3973. DOI: 10.1021/ma202273j.
(90) Swapan K. Ghosh, P. P. D., Dipak Khastgir, Sadhan K. De. Zinc ionomer based on sulfonated maleated styrene-ethylene/ butylene-styrene block copolymer. *Macromolecules Rapid Communication* **199**, *20* (9).
(91) Doan, K. E.; Ratner, M. A.; Shriver, D. F. Synthesis and electrical response of single-ion conducting network polymers based on sodium poly(tetraalkoxyaluminates). *Chemistry of Materials* **1991**, *3* (3), 418-423. DOI: 10.1021/cm00015a012.
(92) Kim, J.-S.; Jackman, R. J.; Eisenberg, A. Filler and percolation behavior of ionic aggregates in styrene-sodium methacrylate ionomers. *Macromolecules* **1994**, *27* (10), 2789-2803.
(93) Salaeh, S.; Das, A.; Wießner, S. Design and fabrication of thermoplastic elastomer with ionic network: A strategy for good performance and shape memory capability. *Polymer* **2021**, *223*. DOI: 10.1016/j.polymer.2021.123699.
(94) Zhou, X.; Guo, B.; Zhang, L.; Hu, G.-H. Progress in bio-inspired sacrificial bonds in artificial polymeric materials. *Chemical Society Reviews* **2017**, *46* (20), 6301-6329.
(95) Creton, C. 50th Anniversary Perspective: Networks and Gels: Soft but Dynamic and Tough. *Macromolecules* **2017**, *50* (21), 8297-8316. DOI: 10.1021/acs.macromol.7b01698.
(96) Zhou, H.; Zhang, M.; Cao, J.; Yan, B.; Yang, W.; Jin, X.; Ma, A.; Chen, W.; Ding, X.; Zhang, G.; et al. Highly Flexible, Tough, and Self-Healable Hydrogels Enabled by Dual Cross-Linking of Triblock Copolymer Micelles and Ionic Interactions. *Macromolecular Materials and Engineering* **2017**, *302* (2), 1600352. DOI: https://doi.org/10.1002/mame.201600352 (acccessed 2023/09/18).
(97) Varley, R. J.; Shen, S.; van der Zwaag, S. The effect of cluster plasticisation on the self healing behaviour of ionomers. *Polymer* **2010**, *51* (3), 679-686. DOI: https://doi.org/10.1016/j.polymer.2009.12.025.
(98) O'Reilly, M. V.; Masser, H.; King, D. R.; Painter, P. C.; Colby, R. H.; Winey, K. I.; Runt, J. Ionic aggregate dissolution and conduction in a plasticized single-ion polymer conductor. *Polymer* **2015**, *59*, 133-143. DOI: https://doi.org/10.1016/j.polymer.2014.12.002.